to destroy cochlear function.[12] Furthermore, it has been reported that testicular tumors are formed in GDNF-overexpressing mice.[19] Therefore, an appropriate regulation system is required to realize the therapeutic benefits of GDNF expression.

Regulated transgene expression has been successfully achieved in various gene therapy experiments using the Tet system.[20–23] Notably, tetracycline derivatives, such as doxycycline (Dox), activate the Tet-on system at doses 100-fold lower than tetracycline. Furthermore, the reverse Tet-responsive transcriptional activator (rtTA) series were improved through the generation of variants called rtTA2s-S2, which showed lower leakiness and better inducibility in HeLa cells and mice.[24,25]

In this study, we describe *in vivo* therapeutic experiments utilizing AAV1 vector–mediated tetracycline-regulated expression of GDNF in cochleae. We demonstrate that AAV1 vector–mediated GDNF expression protects sensory cells in the inner ear from drug-induced degeneration.

RESULTS

Expression and distribution of transgene in the cochlea

AAV1-EGFP or AAV1-GDNF containing either the enhanced humanized green fluorescent protein (*EGFP*) gene or the *GDNF* gene under the control of the CAG (human cytomegalovirus (CMV) immediate-early enhancer and Chicken β-actin promoter) promoter, and the Woodchuck hepatitis virus posttranscriptional regulatory element (WPRE) (Figure 1a), was injected into the cochlea. The GDNF protein level in the perilymph was measured by enzyme-linked immunosorbent assay (Figure 2a). There was a significant increase in GDNF concentration in the cochlea transduced with AAV1-GDNF. The widespread distribution of the GDNF expression was observed in the cochlea, including the spiral ganglion and the inner hair cells (Figure 2b).

To examine the possible transduction of the contralateral ear with the virus diffusion, we analyzed the AAV vector–meditated transgene expression of the rodents with this transduction approach using the optical bioluminescence imaging. Luciferase expression was mainly detected at the injected side of the cochleae (5,370.3 photons/sec/cm²/sr, **Supplementary Figure S1**). Interestingly, the AAV vector also transduced the contralateral ear (876.8 photons/sec/cm²/sr), along with the brain (792.9 photons/sec/cm²/sr). Similar results were obtained with repeated experiments.

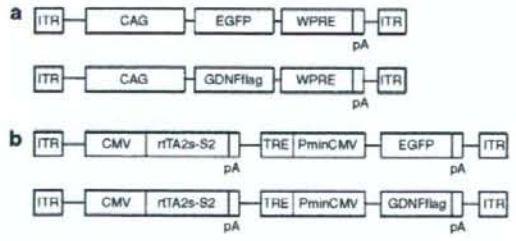

Figure 1 Schematic representation of the viral vectors used in this study. (**a**) An adeno-associated virus 1 (AAV1)-based vector was constructed using the CAG promoter to drive enhanced green fluorescent protein (EGFP) or mouse glial cell line–derived neurotrophic factor (GDNF) with a FLAG tag (GDNFflag). The Woodchuck hepatitis virus posttranscriptional regulatory element (WPRE) was inserted into the 3′ end of the transgene cassette. (**b**) The transactivator rtTA2s-S2 is under the control of the CMV promoter. The minimal CMV promoter (PminCMV) induces transgene expression (EGFP or GDNFflag) in combination with the Tetracycline-responsive element (TRE) and transactivator. CAG, human cytomegalovirus immediate-early enhancer and Chicken β-actin promoter; CMV, cytomegalovirus immediate-early promoter; pA, the simian virus 40 polyadenylation sequences; ITR, inverted terminal repeat from AAV2.

Preservation of the hair cells and spiral ganglion cells in the cochlea

Hair cell loss in the whole-mount cochleae of all the tested rat groups was analyzed by F-actin staining with rhodamine–phalloidin. Figure 3a shows a representative dissection through the second turn of the rat cochlea, in which a full complement of hair cells is revealed by F-actin phalloidin staining. In the vehicle-treated control group, outer hair cells in the base and middle turn were drastically lost after kanamycin treatment (Figure 3b). In the AAV1-GDNF/kanamycin-treated group, successful protection of the hair cells in the cochlea was observed (Figure 3c). In the contralateral cochlea, some of outer hair cells were also protected (Figure 3d). The spiral ganglion cell loss in the basal turn of the cochlea was assessed using 4′,6-diamino-2-phenylindole dihydrochloride staining (Figure 4a and b). Survival of the spiral ganglion cells in the AAV1-GDNF injected cochlea was significantly improved compared to that in the AAV1-EGFP injected cochlea (Figure 4c).

Protection of cochlear function by GDNF

Auditory brain stem response (ABR) recordings of the aminoglycoside-treated animals were performed to examine hearing

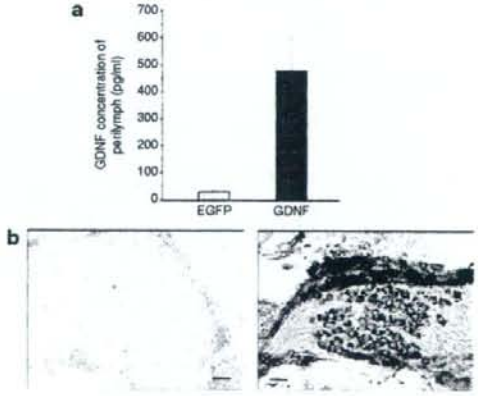

Figure 2 Expression and distribution of transgene in the cochlea. (**a**) Cochlear glial cell line–derived neurotrophic factor (GDNF) expression levels were measured by enzyme-linked immunosorbent assay in the transduced rats. GDNF expression level of the perilymph in the AAV1-GDNF/kanamycin group was significantly higher than that in the control group ($n = 5$, $P < 0.001$). (**b**) Immunohistochemistry was performed to analyze the expression of the GDNFflag in the rat cochlea. The AAV1-EGFP-transduced cochlea was used as a control (left). Cochlear sections were prepared after AAV1-GDNF injection and kanamycin administration. GDNflag expression was detected in the cochlea with an anti-FLAG antibody (right). Scale bar = 25 μm; ×400. AAV1, adeno-associated virus 1; EGFP, enhanced green fluorescent protein.

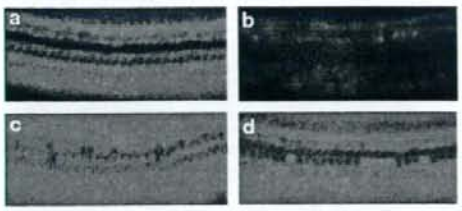

Figure 3 Preservation of the hair cells in the transduced cochlea. Hair cell loss in the cochlea of transduced rats was analyzed by F-actin staining. The dissected samples were dissected from the middle turn of the cochlea. The adeno-asssociated virus 1 (AAV1) vector was injected into the scala tympani of the cochlea prior to 12 days of kanamycin administration. (**a**) The normal cochlea. (**b**) The cochlea from the vehicle-treated ear; the many dark spaces represent the loss of outer hair cells. (**c**) The cochlea from the AAV1-GDNF-transduced ear. (**d**) The cochlea from the contralateral ear of AAV1-GDNF transduced rats. GDNF, glial cell line–derived neurotrophic factor.

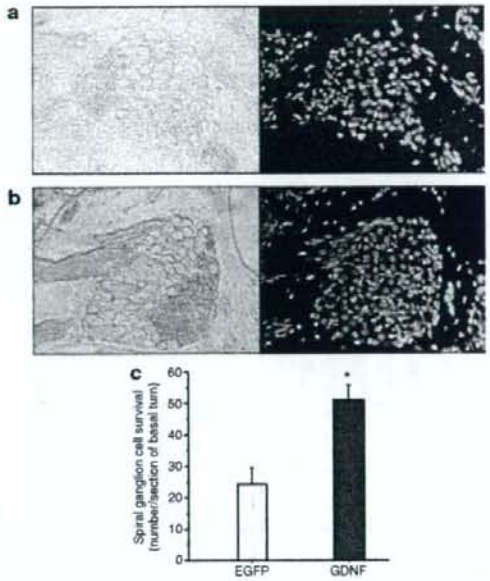

Figure 4 Survival of the spiral ganglion cells in the transduced cochlea. AAV1-GDNF-mediated rescue of the kanamycin-induced damage to the rat spiral ganglion neurons (SGNs): 4′,6-diamino-2-phenylindole dihydrochloride (DAPI) staining was performed on the sections obtained from the rat pretreated with either AAV1-EGFP or AAV1-GDNF, followed by kanamycin injections. (**a**, **b**) Representative photomicrographs of the cryosections showing the basal turn of the cochlear spiral (**a**, AAV1-EGFP; **b**, AAV1-GDNF). (**c**) The number of DAPI-positive large-nucleus cells that exhibited SGN morphology was counted. An asterisk denotes a statistically significant difference between the AAV1-GDNF and AAV1-EGFP-transduced rats (*t*-test, $P < 0.001$). AAV1, adeno-associated virus 1; EGFP, enhanced green fluorescent protein; glial cell line–derived neurotrophic factor.

impairment. At all frequencies tested, both GDNF-transduced and contralateral, untreated ears showed a significant improvement in the threshold shifts compared to the ears transduced with EGFP ($n = 5$, $P < 0.05$) (Figure 5). In the EGFP group, there was

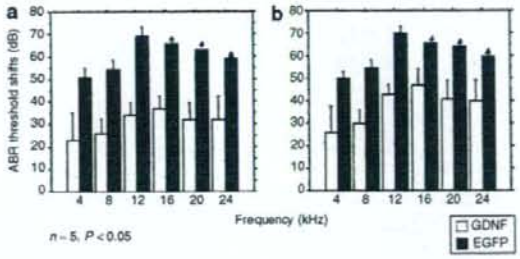

Figure 5 Protection of cochlear function by glial cell line–derived neurotrophic factor GDNF. Auditory brain stem response (ABR) threshold shifts (mean ± SD) of the (**a**) treated and (**b**) untreated ears at each tested frequency in the enhanced green fluorescent protein (EGFP) and GDNF transduced rats. The ABR threshold was measured twice in all the animals. The ears treated with AAV1-GDNF showed a significant improvement in the threshold shifts compared to the ears treated with AAV1-EGFP at all frequencies tested ($n = 5$, $P < 0.05$). Arrows indicate the average ABR thresholds that exceeded the output power of the ABR apparatus. AAV1, adeno-associated virus 1.

no significant difference in the ABR threshold shifts between the transduced and contralateral, untreated cochleae at all frequencies tested. Animals transduced with the AAV1-GDNF demonstrated lower ABR threshold shifts in the injected side compared to the contralateral side (at 12, 16, 20, 24 kHz; $P < 0.05$). These data indicate that both ears were protected even if the AAV1-GDNF was only injected into one ear.

Induced transgene expression

Two hundred and ninety three cells were transduced with the proviral plasmid harboring rtTA2s-S2 and the tetracycline-responsive element (TRE) to express the *EGFP* gene (Figure 1b). In the presence of Dox, a significant level of fluorescence was detected, suggesting that the rtTA2s-S2 system could switch on transcription following Dox treatment (Figure 6a). In contrast, reporter gene expression in the cultured cells was faint in the absence of Dox, indicating a low basal activity *in vitro*. Western blot analysis of GDNF showed that the transgene was induced in the presence of Dox, while no expression was detected in the absence of Dox (Figure 6b).

In vivo induction of GDNF expression and the dose–response to Dox

Enzyme-linked immunosorbent assay analysis of the GDNF expression level in muscle also showed low basal activity and induced expression after Dox treatment (Figure 6c). In the absence of Dox, the expression level of GDNF in the AAV2-S2-GDNF group was as low as that in the phosphate-buffered saline and AAV2-*LacZ* groups. On the other hand, significant increases in the GDNF level were observed in the muscle with increasing amounts of Dox, demonstrating that the rtTA2s-S2 system induces gene expression in a dose-dependent manner.

Inducible GDNF expression in the cochlea

Extensive inducible GDNF transgene expression was confirmed by immunohistochemistry using an anti-FLAG-antibody in the AAV1-S2-GDNF/kanamycin group in the presence of Dox (Figure 7).

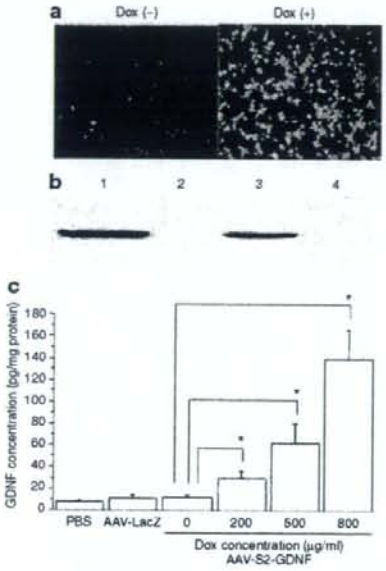

Figure 6 Induction of the transgene expression. (**a**) HEK293 cells were transfected with the proviral plasmid pAAV2-rtTA-S2-TRE-d2EGFP, and the expression of enhanced green fluorescent protein (EGFP) was induced by the doxycycline (Dox) (1 μg/ml). (**b**) Western blot analysis with an anti-FLAG antibody to detect the glial cell line–derived neurotrophic factor (GDNF) expression in the transduced 293 cells with the proviral plasmids. pAAV2-GDNF (lane 1), pAAV2-EGFP (lane 2), pAAV2-rtTA2s-S2-TRE-GDNF with Dox (lane 3), and pAAV2-rtTA2s-S2-TRE-GDNF without Dox (lane 4). (**c**) Dose–response of GDNF in the AAV2-S2-GDNF-injected muscle to the various concentrations of Dox. Mice were injected with phosphate-buffered saline (PBS), AAV2-LacZ, or AAV2-S2-GDNF followed by Dox administered in the drinking water. The mean muscle GDNF concentration in the animals treated with the AAV2-S2-GDNF in the absence of Dox was not significantly different compared to the animals treated with PBS or AAV2-*LacZ* ($P > 0.05$). The GDNF expression levels in the animals transduced with the AAV2-S2-GDNF significantly increased with increasing Dox concentration ($P < 0.05$). AAV1, adeno-associated virus 1.

In contrast, no detectable GDNF expression was observed in the cochlea of the AAV1-S2-GDNF/kanamycin group in the absence of Dox (data not shown).

Protection of cochlear function with induced GDNF expression

To evaluate the adverse effects of the transduction procedure, ABR recordings were performed on kanamycin-free rats after injection of the inducible AAV1-S2-GDNF vectors and Dox administration. At all frequencies tested, no significant increase in the ABR threshold was observed after virus injection (Figure 8a). This result indicates that AAV1 vector injection, transgene expression, and Dox administration did not affect the ABR threshold of the experimental rats. Interestingly, even if AAV1-S2-GDNF was injected into the cochlea of one ear, the cochleas of both ears were protected in the presence of Dox. In particular, the ABR threshold shifts were significantly improved in both the AAV1-S2-GDNF-injected cochlea of the kanamycin-treated rats in the presence of Dox (Figure 8b)

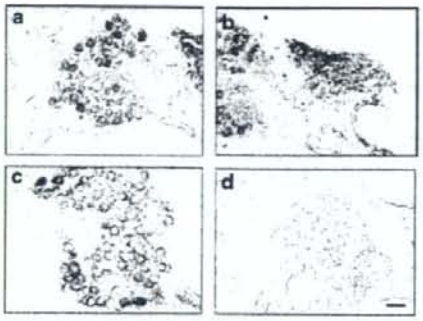

Figure 7 Expression of the GDNFflag in the rat cochlea. (**a**, **b**, **c**) The sections were sampled after the AAV1-S2-GDNF injection into the cochlea in the presence of doxycycline. GDNFflag expression was detected using an anti-FLAG antibody. (**d**) Samples from AAV1-EGFP-inoculated cochlea were analyzed as the negative control. Scale bar = 25 μm; ×400. AAV1, adeno-associated virus 1; GDNF, glial cell line–derived neurotrophic factor; EGFP, enhanced green fluorescent protein.

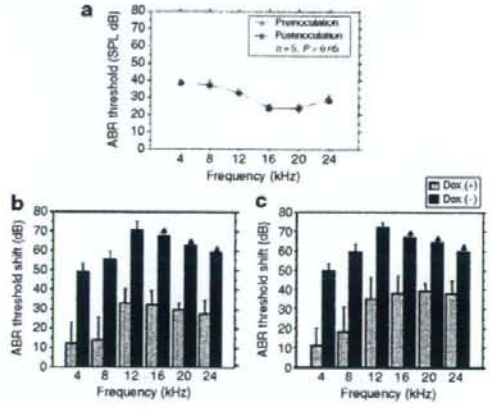

Figure 8 Protection of cochlear function with induced glial cell line–derived neurotrophic factor (GDNF) expression. (**a**) Auditory brain stem response (ABR) thresholds (mean ± SD) at each frequency tested in the AAV1-S2-GDNF-injected rat cochlea in the presence of doxycycline (Dox). No significant difference in the hearing thresholds was observed at each frequency between preinjection and postinjection. SPL, sound pressure level. ABR threshold shifts (mean ± SD) at each tested frequency in the (**b**) transduced or (**c**) nontransduced cochlea with or without Dox. Significant differences in the hearing threshold shifts were observed at each frequency between AAV1-S2-GDNF cochlea in the presence and absence of Dox ($n = 5$, $P < 0.05$). Arrows indicate the average ABR thresholds that exceeded the output power of the ABR apparatus.

and the cochlea of the noninjected contralateral ear (Figure 8c). However, the ABR threshold shifts at all frequencies were significantly lower in the treated group (AAV1-S2-GDNF/kanamycin plus Dox) than in the contralateral, untreated ear.

DISCUSSION

In this study, we showed that both sustained and regulated AAV1-mediated GDNF expression protected the cochlear function of rats from aminoglycoside-induced ototoxicity. Indeed, damaged spiral ganglion cells and hair cells were significantly reduced by

regulated GDNF expression. The ABR monitoring revealed that there was no loss of the cochlear function over the frequencies tested after AAV vector injection and Dox treatment. These data suggest that regulated expression of GDNF in the cochlea efficiently preserves the cochlea from kanamycin-induced ototoxicity.

Among the various viral vector systems, the recombinant AAV-mediated gene transduction system offers several important advantages as a tool for direct somatic gene delivery into the cochlea. These include long-term stable expression of therapeutic genes in a wide variety of postmitotic tissues and minimal vector-related cytotoxicity.[26] In our previous report, we demonstrated the effective transduction of mouse cochleae with the AAV1-based vectors.[7] Generally the therapeutic effectiveness depends on an appropriate concentration and the half-life of the molecules. AAV vector–mediated gene transfer is a promising delivery technique to facilitate a long-term and chronic supply of therapeutic proteins that have a short half-life, such as GDNF. Furthermore, when the CAG promoter is used, efficient transduction activity is observed in the cochlear cells including the inner hair cells and spiral ganglion cells.[27,28]

Our data showed that AAV1-GDNF-mediated transduction of the rat cochleae provided significant protection of the cochlea against aminoglycoside-induced damage. This finding is consistent with previous studies that have used adenovirus-mediated GDNF expression[13,15,16] and demonstrates the feasibility of gene therapy with AAV1-based vectors for drug-induced hearing loss. Although the exact mechanism has not yet been elucidated, antioxidant pathways might be involved in the protective function of GDNF in the inner ear.[29] Free-radical formation following exposure to aminoglycoside is considered one of the major mechanisms to explain the aminoglycoside-related hair cell death.[1,30,31] It has been previously shown that GDNF is endogenously synthesized in the inner hair cells and spiral ganglion cells of the cochlea,[32] and the two known GDNF receptors are present in the spiral ganglion.[17,32,33] In the present study, we inoculated the cochlea with the AAV1 vectors via the round window membrane and detected a high level of transgene expression mainly in the inner hair cells and spiral ganglion cells. The AAV1-mediated GDNF expression pattern was similar to that of the endogenous protein; therefore GDNF supplemented *in situ* can play a substantial role in protection. Although the transduction of the *GDNF* gene was not observed in outer hair cells, GDNF levels in the perilymph of the manipulated cochleae was much higher than in the control cochleae. These cells may respond to the secretion of another growth factor that promotes hair cell survival. Upregulation of GDNF in inner hair cells and spiral ganglion cells following noise also support this concept.[34]

Compared to the vehicle controls, increased cochlear cell survival was observed in the contralateral ears of the AAV1-GDNF group, suggesting that the contralateral cochleae in treated rats were also moderately protected. Expression of the transgene was detected in the contralateral cochlea of the rats after injection with 5×10^{10} genome copies of AAV1 per cochlea (data not shown). AAV can diffuse from one ear to the other via the cerebrospinal fluid in rodents.[35] Therefore, secreted GDNF molecules may also diffuse and exert a protective effect in the opposite ear. Alternatively, GDNF might enhance the neuronal activity (either afferent or efferent) of both ears, protecting both the treated and the contralateral cochlear function. Moreover, since infusion of the vectors into the cochlea forces large amounts of the vectors into the cerebrospinal fluid, any functional effect might be associated with the transduction of the brain. In this context, it is of great interest to know whether the otoprotective effect was achieved by the simple diffusion of the transgene product or direct transduction of the cells in the contralateral ear. To answer this question, we analyzed the local expression of the nonsecretory protein marker in the rodents with this transduction approach. Consequently, we feel that the direct transduction of the cells in the contralateral ear might be involved in the neuroprotection.

The present results showed that AAV-mediated delivery of a Tet-on system was able to control transgene expression. This Tet-on system incorporates the mutant transactivator rtTA2s-S2 and the transgene in which messenger RNA transcription is activated in the presence of an inducer, leading to protein expression. As we showed, the inducible expression of GDNF efficiently protected the cochlear structure and function from kanamycin-induced damage. GDNF was overexpressed in the induced state with the rtTA2s-S2 system, whereas GDNF expression was nearly normal in the non-induced state. In our study, cochlear function was significantly protected from aminoglycoside-induced cochlear damage in the presence of Dox. Although intracochlear injections did not affect physiological cochlear function, intramuscular injections of the vectors expressing Dox-dependent activators may elicit a cellular and humoral response against the transactivator in nonhuman primates.[36–38] The use of tissue-specific promoters that restrict transgene expression to nonprofessional antigen-presenting cells, and the use of AAV vectors, may reduce the induction of a specific T-cell response.[39]

Another attractive feature of the Tet-on system is the high safety profile of the inducer. In our study, Dox was orally administered to the rats to induce GDNF expression. Transgene expression levels were dependent on the dose of Dox, and the dose range of this inducer was below the normal bactericidal treatment levels used in similarly sized animals.[40,41] Furthermore, a Dox regimen in mice that is proportional to a clinically accepted dose of the drug in humans causes a significant induction of transgene expression.

Sequences of antibiotic administration and withdrawal to reverse the Dox induction of therapeutic gene expression were demonstrated in previous studies.[25,42] However, the aminoglycoside-induced hearing impairment model is not an appropriate model for adding and removing the Dox diet because the insulting phase is too short to successively induce and repress the Tet-on system. Furthermore, treatment of age-related hearing loss or genetic hearing loss ideally needs long-term gene expression studies to exclude any adverse events associated with the therapeutic genes.

Efficient control of the tetracycline-regulatory system is based on the specificity of the TetR/tetO interaction and the efficiency and safety of its inducers, such as tetracycline or Dox.[43,44] Mutant tTA2s are composed of one TetR and three repeated oligonucleotides of the VP-16-derived minimal activation domain. In the Tet-on system, rtTA2s-S2 showed a high activating ratio because its background expression level was lower than that of other mutants, such as rtTA2s-M2, which despite having a higher activation potential had also a high initial background.[25] By using the mutant transactivator, Urlinger *et al.* demonstrated that stringent regulation of target genes could be achieved over a range of four to five orders of magnitude

in stably transfected HeLa cells.[24] These regulatory systems could be further optimized to offer several potential advantages. The tetracycline-dependent transcriptional silencer allows tight regulation of transgene expression by eliminating baseline leakage.[20,45] Gene regulation mediated by rtTA2s-S2 was substantially tighter when combined with active silencing by the tetracycline-dependent transcriptional silencer in the non-induced state.[41,46]

Our results show that AAV1-mediated gene transfer is a promising gene delivery approach for the inner ear apparatus. To become an efficient and safe therapeutic method, it will be necessary to improve vector technology to achieve long-term transduction in a fail-safe system. We presented data demonstrating successful AAV-mediated transfer and modulation of transgene expression in the cochlea using a modified Tet-on system. In addition to the need for dosage control of neurotrophic factors, the AAV1 and the Tet-on system maybe useful for the regulation of the expression of other therapeutic gene products in the cochlea. Following further improvements, the rAAV-mediated transduction system may be of potential use for cochlear gene therapy applications in humans.

MATERIALS AND METHODS

Construction and preparation of the plasmids. The AAV vector proviral plasmid pAAV2-CAG-EGFP-WPRE (pAAV2-EGFP) contained the *EGFP* gene under the control of the CAG promoter and the WPRE and was flanked by inverted terminal repeats. A *Bam*HI fragment containing the GDNFflag complementary DNA was subcloned into this plasmid to obtain the pAAV2-CAG-GDNF-WPRE (pAAV2-GDNF) cassette.

The pAAV2-CMV-GDNFflag plasmid with the CMV promoter, the first intron of the human growth hormone gene, and the simian virus 40 polyadenylation signal sequence, were inserted between the inverted terminal repeats of the AAV type 2 genome.[47] The transactivator rtTA2s-S2 complementary DNA in the pUHrT61-1 plasmid (BD Biosciences, San Jose, CA) and the TRE in the pTRE-d2EGFP plasmid (BD Biosciences, CA) were subcloned together into the pAAV2-CMV-GDNFflag plasmid to obtain the AAV vector proviral plasmid pAAV2-rtTA2s-S2-TRE-GDNF. A *Sac*II-*Eco*RI fragment containing the d2EGFP complementary DNA from the pTRE-d2EGFP plasmid (BD Biosciences, CA) was subcloned into this plasmid to create the pAAV2-rtTA2s-S2-TRE-EGFP plasmid (see **Supplementary Materials and Methods**).

Recombinant AAV vector production. The AAV1 vectors were produced as previously described by using a 293-cell transfection protocol[39] with the proviral plasmid pAAV2-EGFP, pAAV2-Luciferase,[48] pAAV2-GDNF, pAAV2-rtTA2s-S2-TRE-EGFP, or pAAV2-rtTA2s-S2-TRE-GDNF; the AAV packaging plasmid pAAV1RepCap; and the adenovirus helper plasmid pAdeno5 using an active gassing system.[49] The recombinant AAV2 expressing the *Escherichia coli* β-galactosidase gene under the control of the CMV promoter (AAV2-LacZ) was generated using the proviral plasmid pAAV-LacZ.[50] (see **Supplementary Materials and Methods**).

In vitro *expression of GDNF.* To detect the *in vitro* expression of the GDNFflag fusion protein, 293 cells were transduced with the AAV1-GDNFflag at 1×10^4 vector genome copies/cell. For the detection of the regulated expression, 293 cells were transduced with the AAV proviral plasmid pAAV2-rtTA2s-S2-TRE-d2EGFP or pAAV2-rtTA2s-S2-TRE-GDNF in the presence or absence of 1 μmol/l Dox-HCl (Sigma, St Louis, MO) (see **Supplementary Materials and Methods**).

Surgical procedures and cochlear perfusions. All animal studies were performed in accordance with the guidelines issued by the committee on animal research at Jichi Medical University. Twenty 5-week-old male Sprague–Dawley rats with normal Preyer's reflexes weighing 130–150 g were utilized (CLEA Japan, Tokyo, Japan). Five-week-old male C57BL/6J mice were utilized for optical bioluminescence imaging. The animals were anesthetized with ketamine (50 mg/kg) and xylazine (5 mg/kg). A postauricular approach was performed to expose the tympanic bony bulla. A small opening (2 mm in diameter) to the tympanic bulla was made by carefully drilling through the bone of the bulla to gain access to the round window membrane. Subsequently, 5 μl of AAV vector solution (AAV1-EGFP, AAV2-Luciferase, or AAV1-GDNF, 5×10^{10} genome copies, $n = 5$ each) was microinjected into the cochlea through the round window for over 10 minutes using a glass micropipette (40 μm in diameter) fitted on a Univentor 801 syringe pump (Serial No. 170182, High Precision Instruments, Univentor Ltd., Malta). The rats were also injected with the AAV1-S2-GDNF in the presence ($n = 5$) or absence ($n = 5$) of Dox. A small plug of muscle was used to seal the cochlea, and the surgical wound was closed in layers and dressed with an antibiotic ointment.

***Transgene expression* in vivo.** The rats were deeply anesthetized and the perilymph was sampled from the inoculated cochlea through the round window. GDNF protein levels were measured using a GDNF Emax ImmunoAssay System (Promega, Madison, WI) according to the manufacturer's instructions. The GDNF expression in the rat cochlea was determined by immunohistochemistry using an anti-FLAG antibody.

AAV2-LacZ or AAV2-S2-GDNF vector (1×10^{10} genome copies) was injected into the quadriceps of the C57BL/6J mice (6 weeks old, CLEA Japan, Tokyo, Japan). The mice were injected with phosphate-buffered saline ($n = 5$) or AAV2-*LacZ* ($n = 5$). Animals treated with various concentrations of Dox were injected with the AAV2-S2-GDNF ($n = 5$ per group). Two weeks after the transduction, animals were deeply anesthetized, and the injected muscle was sampled. The tissue levels of the GDNF protein were measured with an enzyme-linked immunosorbent assay kit (GDNF Emax ImmunoAssay System, Promega, WI), according to the manufacturer's instructions. The levels of GDNF were expressed as pg/mg protein. The assay sensitivity ranged from 16 to 1,000 pg/ml.

Two weeks after the injection of the AAV2-Luciferase, optical bioluminescence imaging was performed using the CCD camera (Xenogen, Alameda, CA). After intraperitoneal injection of reporter substrate D-Luciferin (375 mg/kg body weight), mice were imaged for scans.

Kanamycin administration and ABR assessment. A dose of 333 mg of kanamycin base/kg body weight was obtained by injecting 3 μl/g body weight. Seven days after virus injection, kanamycin was given subcutaneously twice daily for 12 consecutive days. The body weight of the animals was monitored daily to adjust the kanamycin dosages accordingly.

Auditory thresholds were determined by audiometry of evoked ABRs using Tucker-DAVIS Technologies and Scope software (Power Lab; ADInstruments, Coloado Springs, CO). Thresholds were evaluated for each animal prior to the start of the injection procedure and 2 days after the termination of kanamycin treatment. The ABRs were measured as previously described,[7] using a two-way repeated analysis of variance (see **Supplementary Materials and Methods**).

Histological evaluation of the cochlear preservation. Cochlear hair cell loss was determined by F-actin staining. One month after transduction, the presence of the cochlear spiral ganglion neurons was determined by 4′,6-diamino-2-phenylindole dihydrochloride staining to visualize nuclear chromatin. After decalcification, 6 μm mid-modiolus cryosections of the cochleae from each animal were histologically analyzed. The number of spiral ganglion neurons was determined in every third section of the cochlear basal turn from the AAV1-transduced and kanamycin-treated rats (see **Supplementary Materials and Methods**).

Statistical analyses. Results are presented as the means ± SD. Data were statistically analyzed using analysis of variance, paired student's *t*-test (injected versus contralateral sides) or unpaired student's *t*-test (therapy versus control groups) (StatView 5.0 software; SAS Institute, Cary, NC).

ACKNOWLEDGMENTS

The authors thank Avigen. (Alameda, CA) for providing the pAAV-LacZ and pAdeno. We also thank Thomas Hope (Department of Microbiology and Immunology, The University of Illinois at Chicago) for providing pBS II SK+WPRE-B11 and Jun-Ichi Miyazaki (Osaka University Graduate School of Medicine, Osaka, Japan) for pCAGGS. The authors also thank Miyoko Mitsu for her encouragement and technical support. This work was supported in part by grants from the Ministry of Health, Labour and Welfare of Japan (Grants-in-Aid for Scientific Research and grant for 21 Century Centers of Excellence program) and the "High-Tech Research Center" Project for Private Universities (matching fund subsidy, from the Ministry of Education, Culture, Sports, Science, and Technology of Japan). The authors declare no conflict of interest.

SUPPLEMENTARY MATERIAL

Materials and Methods.

Figure S1. Bioluminescence of the transduced cochlea in living mice.

REFERENCES

1. Wu, WJ, Sha, SH and Schacht, J (2002). Recent advances in understanding aminoglycoside ototoxicity and its prevention. *Audiol Neurootol* **7**: 171–174.
2. Hellier, WP, Wagstaff, SA, O'Leary, SJ and Shepherd, RK (2002). Functional and morphological response of the stria vascularis following a sensorineural hearing loss. *Hear Res* **172**: 127–136.
3. Tsue, TT, Oesterle, EC and Rubel, EW (1994). Hair cell regeneration in the inner ear. *Otolaryngol Head Neck Surg* **111**: 281–301.
4. Raphael, Y, Frisancho, JC and Roessler, BJ (1996). Adenoviral-mediated gene transfer into guinea pig cochlear cells *in vivo*. *Neurosci Lett* **207**: 137–141.
5. Ishimoto, S, Kawamoto, K, Kanzaki, S and Raphael, Y (2002). Gene transfer into supporting cells of the organ of Corti. *Hear Res* **173**: 187–197.
6. Okada, T, Nomoto, T, Shimazaki, K, Lijun, W, Lu, Y, Matsushita, T *et al.* (2002). Adeno-associated virus vectors for gene transfer to the brain. *Methods* **28**: 237–247.
7. Liu, Y, Okada, T, Sheykholeslami, K, Shimazaki, K, Nomoto, T, Muramatsu, SI *et al.* (2005). Specific and efficient transduction of cochlear inner hair cells with recombinant adeno-associated virus type 3 vector. *Mol Ther* **12**: 725–733.
8. Lin, LF, Doherty, DH, Lile, JD, Bektesh, S and Collins, F (1993). GDNF: a glial cell line-derived neurotrophic factor for midbrain dopaminergic neurons. *Science* **260**: 1130–1132.
9. Henderson, CE, Phillips, HS, Pollock, RA, Davies, AM, Lemeulle, C, Armanini, M *et al.* (1994). GDNF: a potent survival factor for motoneurons present in peripheral nerve and muscle. *Science* **266**: 1062–1064.
10. Wang, Y, Lin, SZ, Chiou, AL, Williams, LR and Hoffer, BJ (1997). Glial cell line-derived neurotrophic factor protects against ischemia-induced injury in the cerebral cortex. *J Neurosci* **17**: 4341–4348.
11. Keithley, EM, Ma, CL, Ryan, AF, Louis, JC and Magal, E (1998). GDNF protects the cochlea against noise damage. *Neuroreport* **9**: 2183–2187.
12. Shoji, F, Yamasoba, T, Magal, E, Dolan, DF, Altschuler, RA and Miller, JM (2000). Glial cell line-derived neurotrophic factor has a dose dependent influence on noise-induced hearing loss in the guinea pig cochlea. *Hear Res* **142**: 41–55.
13. Suzuki, M, Yagi, M, Brown, JN, Miller, AL, Miller, JM and Raphael, Y (2000). Effect of transgenic GDNF expression on gentamicin-induced cochlear and vestibular toxicity. *Gene Ther* **7**: 1046–1054.
14. Yagi, M, Kanzaki, S, Kawamoto, K, Shin, B, Shah, PP, Magal, E *et al.* (2000). Spiral ganglion neurons are protected from degeneration by GDNF gene therapy. *J Assoc Res Otolaryngol* **1**: 315–325.
15. Hakuba, N, Watabe, K, Hyodo, J, Ohashi, T, Eto, Y, Taniguchi, M *et al.* (2003). Adenovirus-mediated overexpression of a gene prevents hearing loss and progressive inner hair cell loss after transient cochlear ischemia in gerbils. *Gene Ther* **10**: 426–433.
16. Kawamoto, K, Yagi, M, Stover, T, Kanzaki, S and Raphael, Y (2003). Hearing and hair cells are protected by adenoviral gene therapy with TGF-beta1 and GDNF. *Mol Ther* **7**: 484–492.
17. Kuang, R, Hever, G, Zajic, G, Yan, Q, Collins, F, Louis, JC *et al.* (1999). Glial cell line-derived neurotrophic factor. Potential for otoprotection. *Ann NY Acad Sci* **884**: 270–291.
18. Yagi, M, Magal, E, Sheng, Z, Ang, KA and Raphael, Y (1999). Hair cell protection from aminoglycoside ototoxicity by adenovirus-mediated overexpression of glial cell line-derived neurotrophic factor. *Hum Gene Ther* **10**: 813–823.
19. Meng, X, Lindahl, M, Hyvonen, ME, Parvinen, M, de Rooij, DG, Hess, MW *et al.* (2000). Regulation of cell fate decision of undifferentiated spermatogonia by GDNF. *Science* **287**: 1489–1493.
20. Perez, N, Plence, P, Millet, V, Greuet, D, Minot, C, Noel, D *et al.* (2002). Tetracycline transcriptional silencer tightly controls transgene expression after *in vivo* intramuscular electrotransfer: application to interleukin 10 therapy in experimental arthritis. *Hum Gene Ther* **13**: 2161–2172.
21. Regulier, E, Pereira de Almeida, L, Sommer, B, Aebischer, P and Deglon, N (2002). Dose-dependent neuroprotective effect of ciliary neurotrophic factor delivered via tetracycline-regulated lentiviral vectors in the quinolinic acid rat model of Huntington's disease. *Hum Gene Ther* **13**: 1981–1990.
22. Rubinchik, S, Woraratanadharm, J, Yu, H and Dong, JY (2005). New complex Ad vectors incorporating both rtTA and tTS deliver tightly regulated transgene expression both *in vitro* and *in vivo*. *Gene Ther* **12**: 504–511.
23. Pluta, K, Luce, MJ, Bao, L, Agha-Mohammadi, S and Reiser, J (2005). Tight control of transgene expression by lentivirus vectors containing second-generation tetracycline-responsive promoters. *J Gene Med* **7**: 803–817.
24. Urlinger, S, Baron, U, Thellmann, M, Hasan, MT, Bujard, H and Hillen, W (2000). Exploring the sequence space for tetracycline-dependent transcriptional activators: novel mutations yield expanded range and sensitivity. *Proc Natl Acad Sci USA* **97**: 7963–7968.
25. Lamartina, S, Roscilli, G, Rinaudo, CD, Sporeno, E, Silvi, L, Hillen, W *et al.* (2002). Stringent control of gene expression *in vivo* by using novel doxycycline-dependent trans-activators. *Hum Gene Ther* **13**: 199–210.
26. Okada, T, Shimazaki, K, Nomoto, T, Matsushita, T, Mizukami, H, Urabe, M *et al.* (2002). Adeno-associated viral vector-mediated gene therapy of ischemia-induced neuronal death. *Methods Enzymol* **346**: 378–393.
27. Stone, IM, Lurie, DI, Kelley, MW and Poulsen, DJ (2005). Adeno-associated virus-mediated gene transfer to hair cells and support cells of the murine cochlea. *Mol Ther* **11**: 843–848.
28. Liu, Y, Okada, T, Nomoto, T, Ke, X, Kume, A, Ozawa, K *et al.* (2007). Promoter effects of adeno-associated viral vector for transgene expression in the cochlea *in vivo*. *Exp Mol Med* **39**: 170–175.
29. Oppenheim, RW (1997). Related mechanisms of action of growth factors and antioxidants in apoptosis: an overview. *Adv Neurol* **72**: 69–78.
30. Priuska, EM and Schacht, J (1995). Formation of free radicals by gentamicin and iron and evidence for an iron/gentamicin complex. *Biochem Pharmacol* **50**: 1749–1752.
31. Sha, SH and Schacht, J (1999). Stimulation of free radical formation by aminoglycoside antibiotics. *Hear Res* **128**: 112–118.
32. Sariola, M, Hession, C, Worley, D, Carmillo, P, Ehrenfels, C, Walus, L *et al.* (1997). Glial cell line-derived neurotrophic factor-dependent RET activation can be mediated by two different cell-surface accessory proteins. *Proc Natl Acad Sci USA* **94**: 6238–6243.
33. Ylikoski, J, Pirvola, U, Virkkala, J, Suvanto, P, Liang, XQ, Magal, E *et al.* (1998). Guinea pig auditory neurons are protected by glial cell line-derived growth factor from degeneration after noise trauma. *Hear Res* **124**: 17–26.
34. Nam, YJ, Stover, T, Hartman, SS and Altschuler, RA (2000). Upregulation of glial cell line-derived neurotrophic factor (GDNF) in the rat cochlea following noise. *Hear Res* **146**: 1–6.
35. Kho, ST, Pettis, RM, Mhatre, AN and Lalwani, AK (2000). Safety of adeno-associated virus as cochlear gene transfer vector: analysis of distant spread beyond injected cochleae. *Mol Ther* **2**: 368–373.
36. Favre, D, Blouin, V, Provost, N, Spisek, R, Porrot, F, Bohl, D *et al.* (2002). Lack of an immune response against the tetracycline-dependent transactivator correlates with long-term doxycycline-regulated transgene expression in non-human primates after intramuscular injection of recombinant adeno-associated virus. *J Virol* **76**: 11605–11611.
37. Latta-Mahieu, M, Rolland, M, Caillet, C, Wang, M, Kennel, P, Mahfouz, I *et al.* (2002). Gene transfer of a chimeric trans-activator is immunogenic and results in short-lived transgene expression. *Hum Gene Ther* **13**: 1611–1620.
38. Lena, AM, Giannetti, P, Sporeno, E, Ciliberto, G and Savino, R (2005). Immune responses against tetracycline-dependent transactivators affect long-term expression of mouse erythropoietin delivered by a helper-dependent adenoviral vector. *J Gene Med* **7**: 1086–1096.
39. Cordier, L, Gao, GP, Hack, AA, McNally, EM, Wilson, JM, Chirmule, N *et al.* (2001). Muscle-specific promoters may be necessary for adeno-associated virus-mediated gene transfer in the treatment of muscular dystrophies. *Hum Gene Ther* **12**: 205–215.
40. McGee Sanftner, LH, Rendahl, KG, Quiroz, D, Coyne, M, Ladner, M, Manning, WC *et al.* (2001). Recombinant AAV-mediated delivery of a tet-inducible reporter gene to the rat retina. *Mol Ther* **3**: 688–696.
41. Lamartina, S, Silvi, L, Roscilli, G, Casimiro, D, Simon, AJ, Davies, ME *et al.* (2003). Construction of an rtTA2(s)-m2/tts(kid) based transcription regulatory switch that displays no basal activity, good inducibility, and high responsiveness to doxycycline in mice and non-human primates. *Mol Ther* **7**: 271–280.
42. Srour, MA, Fechner, H, Wang, X, Siemetzki, U, Albert, T, Oldenburg, J *et al.* (2003). Regulation of human factor IX expression using doxycycline-inducible gene expression system. *Thromb Haemost* **90**: 398–405.
43. Kistner, A, Gossen, M, Zimmermann, F, Jereck, J, Ullmer, C, Lubbert, H *et al.* (1996). Doxycycline-mediated quantitative and tissue-specific control of gene expression in transgenic mice. *Proc Natl Acad Sci USA* **93**: 10933–10938.
44. Knott, A, Garke, K, Urlinger, S, Guthmann, J, Muller, Y, Thellmann, M *et al.* (2002). Tetracycline-dependent gene regulation: combinations of transregulators yield a variety of expression windows. *Biotechniques* **32**: 796, 798, 800 passim.
45. Rendahl, KG, Quiroz, D, Ladner, M, Coyne, M, Seltzer, J, Manning, WC *et al.* (2002). Tightly regulated long-term erythropoietin expression in vivo using tet-inducible recombinant adeno-associated viral vectors. *Hum Gene Ther* **13**: 335–342.
46. Salucci, V, Scarlto, A, Aurisicchio, L, Lamartina, S, Nicolaus, G, Giampaoli, S *et al.* (2002). Tight control of gene expression by a helper-dependent adenovirus vector carrying the rtTA2(s)-M2 tetracycline transactivator and repressor system. *Gene Ther* **9**: 1415–1421.
47. Wang, L, Muramatsu, S, Lu, Y, Ikeguchi, K, Fujimoto, K, Okada, T *et al.* (2002). Delayed delivery of AAV-GDNF prevents nigral neurodegeneration and promotes functional recovery in a rat model of Parkinson's disease. *Gene Ther* **9**: 381–389.
48. Okada, T, Uchibori, R, Iwata-Okada, M, Takahashi, M, Nomoto, T, Nonaka-Sarukawa, M *et al.* (2006). A histone deacetylase inhibitor enhances recombinant adeno-associated virus-mediated gene expression in tumor cells. *Mol Ther* **13**: 738–746.
49. Okada, T, Nomoto, T, Yoshioka, T, Nonaka-Sarukawa, M, Ito, T, Ogura, T *et al.* (2005). Large-scale production of recombinant viruses by use of a large culture vessel with active gassing. *Hum Gene Ther* **16**: 1212–1218.
50. Okada, T, Mizukami, H, Urabe, M, Nomoto, T, Matsushita, T, Hanazono, Y *et al.* (2001). Development and characterization of an antisense-mediated prepackaging cell line for adeno-associated virus vector production. *Biochem Biophys Res Commun* **288**: 62–68.

Therapeutic Effects of Hepatocyte Transplantation on Hemophilia B

Kohei Tatsumi,[1] Kazuo Ohashi,[2,3,4,5] Midori Shima,[1] Yoshiyuki Nakajima,[2] Teruo Okano,[3] and Akira Yoshioka[1]

Hepatocyte transplantation offers an alternative therapeutic approach in the treatment of liver-related diseases. Hemophilia B is a bleeding disorder lacking factor IX (FIX) production in the liver, and achieving more than 1% coagulation activity results in significant improvement in the quality of life of the patients. The aim of this study was to investigate the efficacy of hepatocyte transplantation in the mouse model of hemophilia B. We transplanted isolated normal mouse hepatocytes into the liver of FIX knock-out mice. In some recipient mice, additional hepatocyte transplantations were performed 15 days after the first transplant. The recipient plasma FIX activities increased at 1% to 2% and persisted throughout the experimental period. An additional increase was achieved by the repeated transplantation. Close correlation between FIX messenger RNA levels of the liver and plasma FIX activity levels was observed. These results demonstrate that hepatocyte transplantation can provide therapeutic benefits in the treatment of hemophilia B.

Keywords: Hepatocyte transplantation, Hemophilia B, Coagulation factor IX, Experimental transplantation.

(*Transplantation* 2008;86: 167–170)

Hemophilia B, a recessive X-chromosome linked congenital bleeding disorder, is caused by a failure in the production of coagulation factor IX (FIX) (*1*). The only treatments that are currently available are the replacement therapy with FIX concentrates from plasma-derived or recombinant protein sources (*2*). This treatment modality is inefficient and expensive, because of the requirement of life-long and frequent intravenous infusion of FIX concentrates. Although the gene therapy has been actively studied over the past decade to establish a novel therapy that could provide longer acting and safer production of FIX (*3*), recent clinical trials have yet to conclusively shown long-term therapeutic benefits (*4, 5*). One potential approach that may provide the FIX producing ability in hemophilia B is a whole liver transplantation, because FIX is predominantly produced in the liver (*6–8*). However, the establishment of organ transplantation as a common therapy is hampered by a worldwide shortage of donor livers. Provided that some portion of the donated liver can be used for the isolation of individual hepatocytes, this donor shortage would no longer be a major issue. This is an important point, because the cell type responsible for synthesizing coagulation FIX is the hepatocyte (*9*). Therefore, a cell-based therapy using isolated hepatocytes could provide a therapeutic approach in the treatment of hemophilia B. Hepatocyte transplantation has been recently performed in several countries for various inherited disorders of hepatic metabolism and acute liver failure (*10, 11*). In bleeding disorder, hepatocyte transplantation was applied in the clinics by Dhawan et al. (*12*), who described therapeutic benefits in two patients suffering with congenital factor VII deficiency. Our group has recently shown applying a tissue engineering approach using primary hepatocytes could successfully provide therapeutic effects in hemophilia A mice (*13*). However, the effect of hepatocyte transplantation to treat hemophilia B has yet to be experimentally documented in animals or in the clinics to the best of our knowledge. For this reason, this study was designed to investigate the efficacy of hepatocyte transplantation on hemophilia B.

Hepatocytes were isolated from C57Bl/6 wild-type mice using a collagenase perfusion method as previously described (*13–16*). The recipient FIX knock-out (FIX-KO) mice, syngeneic to donor mice (*17*), were transplanted with the isolated hepatocytes (1.5×10^6 cells in 200 μL) into the liver through the inferior pole of the spleen (n=25). As an experimental control, several FIX-KO mice received sham operation (n=7). To avoid excessive surgical procedure-related bleeding, all FIX-KO mice received intraperitoneal injection of 0.5 mL pooled normal mouse plasma 30 min before abdominal surgery (*18*). All procedures were successfully carried out without any issues related to bleeding and all of the mice survived throughout the experimental period. At days 5, 10, and 15, some of the mice were killed for histologic and messenger RNA (mRNA) analyses (n=7, 5, and 4, at each time point, respectively). All sham-operated mice were killed at day 15.

Blood samples were periodically obtained from retro-orbital plexus of the experimental mice. After anticoagulated with 0.1 volume of 3.8% sodium citrate, blood samples were centrifuged, and plasma samples were stored at −80°C until being analyzed. The plasma FIX activity (FIX:C) was quanti-

This work was supported by grants form AIDS Research from the Ministry of Health, Labor and Welfare of Japan (A.Y.) and grant-in-Aid (18591957) (K.O.) and Special Coordination Funds for Promoting Science and Technology (K.O., T.O.), and from the Ministry of Education, Culture, Sports, Science and Technology (MEXT), Japan.

[1] Department of Pediatrics, Nara Medical University, Kashihara, Nara, Japan.
[2] Department of Surgery, Nara Medical University, Kashihara, Nara, Japan.
[3] Institute of Advanced Biomedical Engineering and Science, Tokyo Women's Medical University, Shinjuku-ku, Tokyo, Japan.
[4] Department of Gastroenterological Surgery Tokyo Women's Medical University, Tokyo, Japan.
[5] Address correspondence to: Kazuo Ohashi, M.D., Ph.D., Institute of Advanced Biomedical Engineering and Science, Tokyo Women's Medical University, 8-1 Kawada-cho, Shinjuku-ku, Tokyo 162-8666, Japan.
E-mail: ohashi@abmes.twmu.ac.jp

Received 8 November 2007. Revision requested 11 December 2007.
Accepted 2 April 2008.

ISSN 0041-1337/08/8601-167
DOI: 10.1097/TP.0b013e31817b9160

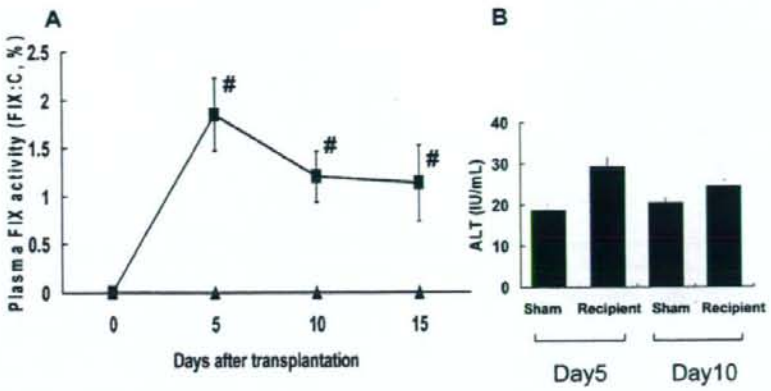

FIGURE 1. Plasma FIX activity (FIX:C) and alanine aminotransferase (ALT) levels of FIX-KO mice after hepatocyte transplantation. (A) FIX:C levels in plasma obtained from FIX-KO mice after hepatocyte transplantation (1.5×10^6 cells/mouse) into the liver (■; n=25, 18, and 13 at day 5, 10, and 15, respectively) or sham operation (▲; n=7 at all time points). Pooled normal mouse plasma was used as a standard. #*P* less than 0.05 between groups. (B) Plasma ALT levels of FIX-KO mice following hepatocyte transplantation (n=25 and 18) or sham operation (n=7) at day 5 and 10 of the experiment.

fied by 1-stage clotting assay based on the activated partial thromboplastin time using human FIX-deficient plasma. Normal mouse plasma was used as FIX:C standard. Each measurement was reported after subtraction of the preoperational baseline FIX:C levels. As a result, FIX:C of recipient mice increased to more than 1% and were stably maintained throughout the experimental period (Fig. 1A). The FIX:C levels were significantly higher in the recipient mice when compared with the levels in the sham-operated mice at every time point examined. At day 5, recipient mice showed a small, but insignificant increase in plasma alanine aminotransferase after the transplantation (n=25) compared with the sham-operated mice (n=7). The slight increase in the alanine aminotransferase levels were found to be declined back toward baseline levels at day 10 (Fig. 1B). These results indicated that hepatocyte transplantation into hemophilia B mice could provide a therapeutic effect by producing FIX from the engrafted donor hepatocytes without significant liver injuries.

Histologic detection of transplanted and engrafted hepatocytes was performed by fluorescence in situ hybridization analysis using mouse Y-chromosome specific probe on sections of female FIX-KO recipient liver that received male hepatocytes. The presence of hepatocytes with Y-chromosome signals were confirmed, indicating the transplanted hepatocytes engrafted into the liver parenchyma (figure not shown). It is also important to note that any cell fusion events were not observed.

To enhance the therapeutic production of FIX in the recipient mice, a repeat transplantation of isolated hepatocytes was performed 15 days after the initial procedure in some recipients by infusing 1.2×10^6 hepatocytes into the upper pole of the spleen (n=4). The other remaining recipients (n=5) were examined with only a single transplantation procedure. As shown in Figure 2, the FIX:C values of the FIX-KO mice at day 25 (10 days after the second transplantation) were $0.94\%\pm0.05\%$ and $1.85\%\pm0.09\%$ in the single- and double-transplanted recipient mice, respectively ($P=0.038$). Similar increases in FIX:C were also observed at day 35 (20 days after the second transplantation) in the double-transplanted group. These data clearly demonstrated that increasing therapeutic effects could be obtained with a repeated transplantation.

We also examined whether the engrafted hepatocytes were capable of transcribing FIX mRNA in the recipient mouse livers. Because shunting of the hepatocytes into the lung had been described in the previous experimental studies (*19*), we also investigated FIX mRNA levels in the lung. Total RNA was extracted from liver, lung, and spleen. Total RNA (1 μg) was reverse transcribed, and the first-strand complementary DNA samples were subjected to quantitative real-time polymerase chain reaction amplification for mouse FIX gene and β-actin gene. Serial dilutions of complementary DNAs of normal mouse liver were used to generate the standard amplification curves. As shown in Figure 3(A), an abundant level of FIX mRNA was detected in the liver, with even higher mRNA expression detected in the livers manipulated with the repeated transplantation. No FIX mRNA signal was detected in the lungs in any of the mouse groups. Incremental expression of FIX was detected in the spleen of single and double hepatocyte transplanted mice, but the levels were markedly lower compared with the livers. We examined the relationship between the FIX:C levels and the liver FIX mRNA levels, and found a direct positive correlation between the two parameters ($R^2=0.7214$) (Fig. 3B).

Furthermore, we assessed the development of neutralizing antibodies against FIX (FIX inhibitor) by Bethesda method using plasma obtained at killing (*20*). Detectable levels (>0.5 Bethesda U/mL) of FIX inhibitor was not measured

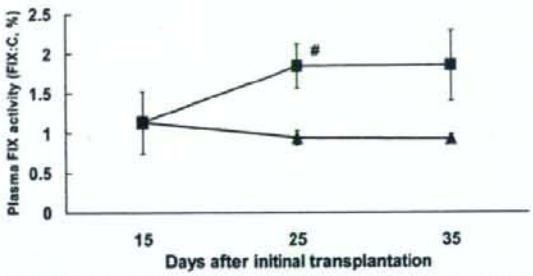

FIGURE 2. Effect of repeated hepatocyte transplantation on plasma FIX:C levels in hemophilia B mice. At day 15, some recipient FIX-KO mice received the second transplantation procedure using 1.2×10^6 hepatocytes (■; n=4), whereas remaining five recipient mice did not receive the second procedure (initial transplantation only, ▲; n=5). #*P* less than 0.05 between groups.

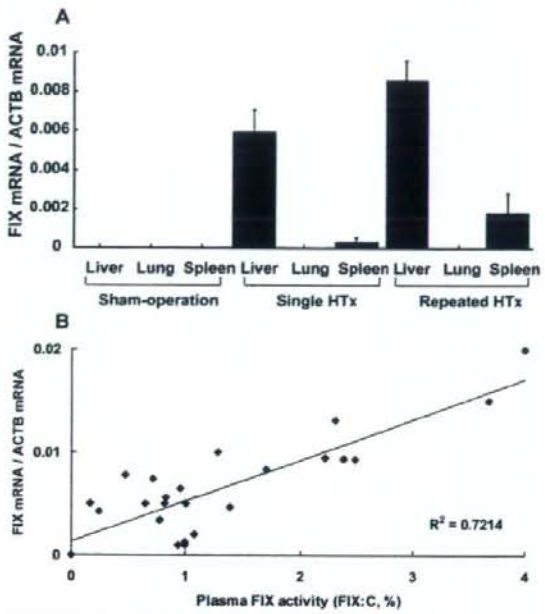

FIGURE 3. Functional engraftment of hepatocytes determined by FIX mRNA expression in the recipient mice. (A) Expression levels of FIX mRNA were determined by quantitative real-time reverse-transcriptase polymerase chain reaction in the liver, spleen, and lung from three experimentally manipulated groups: (1) single hepatocyte transplantation (n=21); (2) repeated hepatocyte transplantation (n=4); and (3) sham-operation (control) (n=7). Each of the FIX mRNA expression values were normalized to a housekeeping gene, β-actin. (B) Relationship between plasma FIX:C levels and FIX mRNA expression levels in the liver of recipient mice. The FIX:C levels of plasma obtained on the day of animal sacrifice were found to correlate with the relative FIX mRNA levels determined in (A) (R^2=0.7214).

in any of recipient mice. This demonstrates that bioengineered FIX produced from the transplanted hepatocytes does not associate with the development of FIX inhibitors.

To investigate the long-term engraftment of hepatocytes, we performed an another set of single transplantation experiment for 12 weeks (n=6), and confirmed long-term persistency of the increased FIX activities at 0.92%±0.22%, 0.78%±0.22%, 0.78%±0.22%, and 0.83%±0.17% at week 2, 4, 8, and 12, respectively.

The present study confirmed the proof-concept feasibility of hepatocyte transplantation as an alternative therapy to treat hemophilia B. The functional engraftment of transplanted hepatocytes within the recipient livers was confirmed by fluorescence in situ hybridization analyses, FIX mRNA expression, and the secretion of functional FIX into the blood circulation. To acquire the proper hemostatic activity, synthesized coagulation FIX requires several posttranscriptional modification steps within the hepatocytes, including cleavage and removal the prepro leader sequence of 46 amino-acids, and γ-carboxylation of the first 12 glutamic acid residues (*21*). For this reason, primary hepatocytes would be more appropriate for transplantation to produce coagulation factors in hemophilia B than other possible types of genetically modified cells expressing FIX.

Previous studies have shown that engrafted hepatocytes within the livers are able to proliferate in response to the regeneration signals occurred by surgical hepatectomy or chronic liver injuries (*22, 23*). Using primary hepatocytes, our group has developed several innovative approaches to create a functional liver system under the kidney capsule or in subcutaneous locations (*13, 15, 16, 24, 25*), and we have clearly demonstrated that these ectopically engrafted hepatocytes also possess the ability for proliferation (*13, 16, 26*). This would be a significant benefit in the use of these hepatocytes, because most of the adult hemophilia B patients presented with chronic hepatitis B and/or C viral infection as a result of treatments with blood-borne contaminated plasma-derived FIX concentrates. Although portion of the transplanted hepatocytes would be infected with hepatitis viruses in the mean time, it would be reasonable to speculate that engrafted hepatocytes will proliferate and expand, which would further increase the therapeutic effects.

In conclusion, the present studies described the feasibility and safety of hepatocyte transplantation as a treatment modality for hemophilia B. Current therapies to treat hemophilia have been confounded with problems, and the present findings represent an important step toward establishing an alternative therapeutic approach for the treatment of not only hemophilia, but other similar genetic disorders affecting the liver.

ACKNOWLEDGMENTS

The authors thank Yuichi Komai, Yuka Bessho, and Sanae Taminishi (Department of Pediatrics, Nara Medical University) for their technical assistance, and Dr. Frank Park (Medical College of Wisconsin) for his critical reading of the manuscript.

REFERENCES

1. Bolton-Maggs PH, Pasi KJ. Haemophilias A and B. *Lancet* 2003; 361: 1801.
2. Manco-Johnson MJ, Abshire TC, Shapiro AD, et al. Prophylaxis versus episodic treatment to prevent joint disease in boys with severe hemophilia. *N Engl J Med* 2007; 357: 535.
3. Nathwani AC, Davidoff AM, Tuddenham EG. Prospects for gene therapy of haemophilia. *Haemophilia* 2004; 10: 309.
4. Manno CS, Chew AJ, Hutchison S, et al. AAV-mediated factor IX gene transfer to skeletal muscle in patients with severe hemophilia B. *Blood* 2003; 101: 2963.
5. Manno CS, Pierce GF, Arruda VR, et al. Successful transduction of liver in hemophilia by AAV-Factor IX and limitations imposed by the host immune response. *Nat Med* 2006; 12: 342.
6. Gordon FH, Mistry PK, Sabin CA, et al. Outcome of orthotopic liver transplantation in patients with haemophilia. *Gut* 1998; 42: 744.
7. Ko S, Tanaka I, Kanehiro H, et al. Preclinical experiment of auxiliary partial orthotopic liver transplantation as a curative treatment for hemophilia. *Liver Transpl* 2005; 11: 579.
8. Merion RM, Delius RE, Campbell DA, Jr, et al. Orthotopic liver transplantation totally corrects factor IX deficiency in hemophilia B. *Surgery* 1988; 104: 929.
9. Boost KA, Auth MK, Woitaschek D, et al. Long-term production of major coagulation factors and inhibitors by primary human hepatocytes in vitro: perspectives for clinical application. *Liver Int* 2007; 27: 832.
10. Fisher RA, Strom SC. Human hepatocyte transplantation: Worldwide results. *Transplantation* 2006; 82: 441.
11. Ohashi K, Park F, Kay MA. Hepatocyte transplantation: Clinical and experimental application. *J Mol Med* 2001; 79: 617.
12. Dhawan A, Mitry RR, Hughes RD, et al. Hepatocyte transplantation for inherited factor VII deficiency. *Transplantation* 2004; 78: 1812.

13. Ohashi K, Waugh JM, Dake MD, et al. Liver tissue engineering at extrahepatic sites in mice as a potential new therapy for genetic liver diseases. *Hepatology* 2005; 41: 132.
14. Berry MN, Friend DS. High-yield preparation of isolated rat liver parenchymal cells: A biochemical and fine structural study. *J Cell Biol* 1969; 43: 506.
15. Ohashi K, Kay MA, Kuge H, et al. Heterotopically transplanted hepatocyte survival depends on extracellular matrix components. *Transplant Proc* 2005; 37: 4587.
16. Ohashi K, Kay MA, Yokoyama T, et al. Stability and repeat regeneration potential of the engineered liver tissues under the kidney capsule in mice. *Cell Transplant* 2005; 14: 621.
17. Lin HF, Maeda N, Smithies O, et al. A coagulation factor IX-deficient mouse model for human hemophilia B. *Blood* 1997; 90: 3962.
18. Snyder RO, Miao C, Meuse L, et al. Correction of hemophilia B in canine and murine models using recombinant adeno-associated viral vectors. *Nat Med* 1999; 5: 64.
19. Schneider A, Attaran M, Gratz KF, et al. Intraportal infusion of 99mtechnetium-macro-aggregrated albumin particles and hepatocytes in rabbits: Assessment of shunting and portal hemodynamic changes. *Transplantation* 2003; 75: 296.
20. Kasper CK, Pool JG. Letter: Measurement of mild factor VIII inhibitors in Bethesda units. *Thromb Diath Haemorrh* 1975; 34: 875.
21. Arruda VR, Hagstrom JN, Deitch J, et al. Posttranslational modifications of recombinant myotube-synthesized human factor IX. *Blood* 2001; 97: 130.
22. Kokudo N, Ohashi K, Takahashi S, et al. Effect of 70% hepatectomy on DNA synthesis in rat hepatocyte isograft into the spleen. *Transplant Proc* 1994; 26: 3464.
23. Zhang H, Miescher-Clemens E, Drugas G, et al. Intrahepatic hepatocyte transplantation following subtotal hepatectomy in the recipient: A possible model in the treatment of hepatic enzyme deficiency. *J Pediatr Surg* 1992; 27: 312.
24. Ohashi K, Marion PL, Nakai H, et al. Sustained survival of human hepatocytes in mice: A model for in vivo infection with human hepatitis B and hepatitis delta viruses. *Nat Med* 2000; 6: 327.
25. Yokoyama T, Ohashi K, Kuge H, et al. In vivo engineering of metabolically active hepatic tissues in a neovascularized subcutaneous cavity. *Am J Transplant* 2006; 6: 50.
26. Ohashi K, Yokoyama T, Yamato M, et al. Engineering functional two- and three-dimensional liver systems in vivo using hepatic tissue sheets. *Nat Med* 2007; 13: 880.

Biochemical and Biophysical Research Communications 374 (2008) 106–110

Contents lists available at ScienceDirect

Biochemical and Biophysical Research Communications

journal homepage: www.elsevier.com/locate/ybbrc

Reference gene selection for real-time RT-PCR in regenerating mouse livers

Kohei Tatsumi [a], Kazuo Ohashi [b,*], Sanae Taminishi [a], Teruo Okano [b], Akira Yoshioka [a], Midori Shima [a]

[a] Department of Pediatrics, Nara Medical University, 840 Shijo-cho, Kashihara, Nara 634-8522, Japan
[b] Institute of Advanced Biomedical Engineering and Science, Tokyo Women's Medical University, 8-1 Kawada-cho, Shinjuku-ku, Tokyo 162-8666, Japan

ARTICLE INFO

Article history:
Received 19 June 2008
Available online 3 July 2008

Keywords:
Liver regeneration
Hepatocyte proliferation
Partial hepatectomy
Housekeeping gene
Real-time RT-PCR
GeNorm
NormFinder
Mouse
PPIA
TBP

ABSTRACT

The liver has an intrinsic ability to undergo active proliferation and recover functional liver mass in response to an injury response. This regenerative process involves a complex yet well orchestrated change in the gene expression profile. To produce accurate and reliable gene expression of target genes during various stages of liver regeneration, the determination of internal control housekeeping genes (HKGs) those are uniformly expressed is required. In the present study, the gene expression of 8 commonly used HKGs, including GAPDH, ACTB, HPRT1, GUSB, PPIA, TBP, TFRC, and RPL4, were studied using mouse livers that were quiescent and actively regenerating induced by partial hepatectomy. The amplification of the HKGs was statistically analyzed by two different mathematical algorithms, geNorm and NormFinder. Using this method, PPIA and TBP gene expression found to be relatively stable regardless of the stages of liver regeneration and would be ideal for normalization to target gene expression.

The process of liver regeneration is a crucial intrinsic event by which the liver is able to recover from a loss of functional hepatic mass following injuries due to either surgical resection, or toxic, chemical or viral-based challenges [1,2]. The molecular events that are involved in the liver regeneration process are very complex, and the altered gene expressions ultimately orchestrate the integration of these distinct pathways to promote the regenerative biological response. Multiple studies have elucidated potential mechanistic pathways that may be involved in the process of liver regeneration, but many aspects of this phenomenon in terms of its gene expression profiles and its associated functional phenotypes remain to be further elucidated.

Among currently available methods to analyze gene expression profiles, reverse transcriptase coupled to real-time polymerase chain reaction (real-time RT-PCR) has recently been shown to be more efficient and reliable compared to the other methods [3]. To accurately quantify gene expression, one method is to normalize the target unknown gene expression level to an endogenously expressed reference gene(s), which are frequently housekeeping genes (HKGs). The ideal HKGs should be expressed at a constant level regardless of the liver regeneration status, otherwise the normalization using particular HKGs will lead to erroneous gene expression profiles of the target gene of interest. Due to the rapid and differential phenotypic changes during liver regeneration process, it is crucial to determine HKGs that remain unaltered throughout the regenerative time period, which generally is terminated by day 5 [2].

Statistical algorithms such as geNorm [4] and NormFinder [5] have been previously developed to evaluate the suitability of reference HKGs for use as a normalization marker following quantitative RT-PCR data in a given set of biological samples. Using these methods of statistical analysis, various HKGs have been recently assessed to determine their level of expression under specific conditions [6,7].

In the present study, we induced liver regeneration in mice using the most commonly used experimental procedure to promote hepatocyte proliferation, known as the 2/3 partial hepatectomy (PHx) [8]. Using this model of liver regeneration, the gene expression levels of 8 commonly used HKGs (GAPDH, ACTB, HPRT1, GUSB, PPIA, TBP, TFRC, and RPL4) and 2 liver-expressing target genes were investigated in quiescent and actively proliferating livers at different time points following PHx. The RT-PCR results were subsequently analyzed by two computer programs, geNorm and NormFinder, to select the best candidate reference gene during the liver regenerative process. To our knowledge, the present study describes the first systematic study to examine a series of HKGs to determine their utility as reference markers to evaluate the expression levels of target genes in regenerating mouse livers.

* Corresponding author. Fax: +81 3 3359 6046.
E-mail address: ohashi@abmes.twmu.ac.jp (K. Ohashi).

0006-291X/$ - see front matter © 2008 Elsevier Inc. All rights reserved.
doi:10.1016/j.bbrc.2008.06.103

Materials and methods

Animals. A total of 25 female wild-type C57BL/6 mice, 10–12 weeks old, were used in this study. Experimental protocols were developed in accordance with the guidelines outlined by our local animal committee located at Nara Medical University. Mice were placed in cages within a temperature-controlled room having a 12-h light/dark cycle (8:00 AM lights on/8:00 PM lights off).

2/3 Partial hepatectomy (PHx). The stimuli for liver regeneration was induced by a 2/3 partial hepatectomy on the C57BL6 wild-type mice ($n = 25$) as described previously [8–11]. The hepatectomy was performed at within a specified time window (between 8:00 and 10:00 AM) in order to minimize the circadian rhythm variations that may influence the speed and peak of the regenerative activity [12]. The liver lobes that were removed from each mouse at the time of hepatectomy were used as control liver samples in the quiescent state ($n = 25$). The mice were sacrificed at different time points (1, 2, and 5 days after hepatectomy; $n = 9$, 8, and 8, respectively) at which time the remainder of the liver lobes were harvested to determine the gene expression at different temporal points of liver regeneration.

RNA isolation and quality controls. Total RNA was extracted from each liver sample using the RNeasy Mini Kit (QIAGEN, Hilden, Germany). DNaseI was used to digest and remove genomic DNA contamination. The RNA concentration of each sample was measured at a wavelength of 260 nm (A260). The purity of extracted total RNA was determined by the A260/A280 ratio. The real-time RT-PCR analyses were only performed on samples that had A260/A280 ratios between 1.9 and 2.1. The integrity of RNA samples was confirmed by electrophoresis on a 1% agarose gel.

Reverse transcription (RT) coupled quantitative real-time PCR. Total RNA (1 μg) was reverse-transcribed using oligo $d(T)_{16}$ primers and Omniscript RT Kit (QIAGEN). First-strand cDNA samples were subjected to quantitative PCR amplification using the PRISM 7700 Sequence Detector (Applied Biosystems Japan, Tokyo, Japan). Each of the liver cDNAs was determined for the expression levels of 8 commonly used housekeeping genes (HKGs) and two target genes as shown in Table 1. TaqMan probes and primers were chosen from the TaqMan Gene Expression Assay (Applied Biosystems) (Table 1). All of the PCR cycling conditions were 10 min at 95 °C, followed by 40 cycles of 15 s at 95 °C, and 1 min at 60 °C. For quantification of gene expression, the cDNAs derived from pooled normal mouse livers were used to generate the reference standard curves.

Statistical analysis and determination of appropriate HKGs by geNorm and NormFinder. Significant differences between the non-normalized gene expression levels of quiescent and regenerating liver samples were analyzed by two-tailed Mann–Whitney *U*-test using Excel with ystat2006 software (Igakutosyosyuppan, Tokyo, Japan). $P < 0.05$ was considered significant. For stability comparisons of candidate reference genes, two additional validation software programs, geNorm (http://medgen.ugent.be/~jvdesomp/genorm/) [4], and NormFinder (http://www.mdl.dk/publicationsnormfinder.htm) [5] were used.

Results

RNA quality control

The mean A260/280 ratio of the extracted RNA of the 25 quiescent and 25 regenerating livers averaged 2.02 ± 0.09 (ranging from 1.95 to 2.10), reflecting the purity and protein-free nature of the RNA. The RNA integrity was characterized by the 28 S/18 S ratio on a 1% agarose gel, and the ratios of all samples were >1.0.

Non-normalized expression levels of candidate reference genes

Non-normalized gene expression levels of 8 candidate HKGs were quantified, and the data was reported as comparative ratio to the day 0 samples. As shown in Fig. 1, the expression levels of GAPDH, ACTB, GUSB, PPIA, and TFRC were significantly higher at days 1 and/or 2 after the hepatectomy, and tended to decrease back towards basal levels by day 5. The *P* values from day 1, 2, and 5 compared to the day 0 values are as follows: GAPDH: 0.007 (day 1), 0.195 (day 2), and 0.46 (day 5), ACTB: 0.053, 0.0004, and 0.649, GUSB: 0.158, 0.004, and 0.051, PPIA: 0.028, 0.0002, and 0.125, and TFRC: 0.758, 0.006, and 0.074. HPRT1 expression was also significantly upregulated at day 2, but the upregulated levels persisted through to day 5. The *P* values of day 1, 2, and 5 compared to the day 0 values were 0.065, 0.001, and 0.017, respectively. In marked contrast, expression levels of TBP and RPL4 genes did not show any significant differences between day 0 with the other days 1, 2, and 5; the *P* values were as follows: TBP: 0.644, 0.23, and 0.35; and RPL4: 0.073, 0.249, and 0.258, respectively. These indicated that the gene expression levels of TBP and RPL4 were constant during the liver regeneration regardless of the time point after partial hepatectomy.

Statistical validation of an appropriate reference gene by geNorm and NormFinder

To analyze and provide a rank order of the 8 candidate HKGs in the quiescent and regenerating liver samples, we utilized geNorm

Table 1
Description of housekeeping gene (HKG) and target gene primers used in the quantitative RT-PCR assay

Symbol	Gene name	Function	Assay ID	Amplicon length (bp)
Housekeeping genes				
GAPDH	Glyceraldehyde-3-phosphate dehydrogenase	Glycolytic enzyme	Mm99999915_g1	107
ACTB	Actin, beta	Cytoskeletal structural protein	Mm00607939_s1	115
HPRT1	Hypoxanthine phosphoribosyltransferase	Purine synthesis in salvage pathway	Mm03024075_m1	131
GUSB	Glucuronidase, beta	Glycoside hydrolases cleaving glucuronides	Mm00446953_m1	76
PPIA	Peptidylprolyl isomerase A	Catalyzing the *cis-trans* isomerization of proline imidic peptide bonds in oligopeptides and accelerating the folding of proteins	Mm02342430_g1	148
TBP	TATA box binding protein	General RNA polymerase II transcription factor	Mm00446973_m1	73
TFRC	Transferrin receptor	Carrier protein for transferrin	Mm00441941_m1	66
RPL4	Ribosomal protein L4	Component of the 60S subunit of ribosome	Mm00834993_g1	129
Target genes				
OTC	Ornithine carbamoyltransferase	Enzyme catalyzing the reaction of urea cycle	Mm00493267_m1	102
AAT	α1-antitrypsin	Glycoprotein functioning as serum trypsin inhibitor	Mm00522856_m1	58

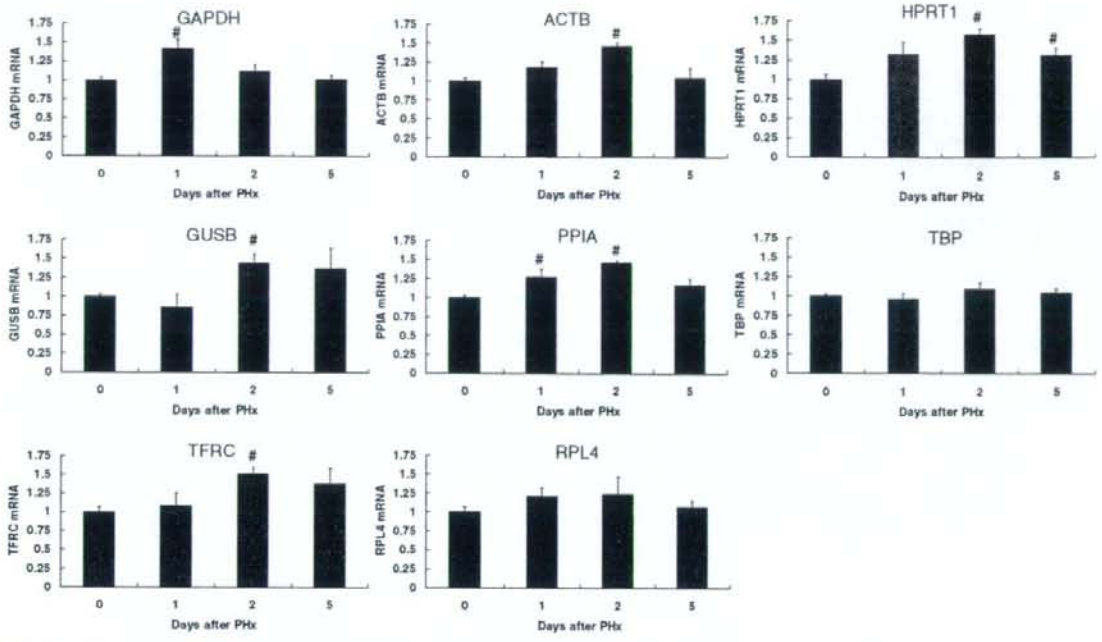

Fig. 1. The expression levels of 8 candidate HKGs in mouse livers. Non-normalized expression levels of the 8 HKGs of mouse livers under quiescent and regenerating status. The liver lobes removed at the time of hepatectomy were used as liver samples under quiescence status (day 0, $n = 25$). The remaining liver lobes obtained 1, 2, or 5 days after hepatectomy were used as samples to study the different stages of regeneration ($n = 9$, 8, and 8, respectively). The data was expressed as a comparative ratio to the day 0 samples, and represented as the mean ± SEM. $^{\#}P < 0.05$ vs day 0.

software. The geNorm is a statistical algorithm that was designed to determine the measure of stability (M) for all of the candidate genes based on the geometric averaging of multiple control genes, as well as the mean pairwise variation of a gene from all other control genes in a given set of samples [4].

The geNorm program relies on the principle that the expression ratio of two ideal internal control genes is identical in all of the samples regardless of the experimental condition. The genes with the lowest M values will be considered to have the most stable expression across time in the quiescent and regenerating livers obtained at days 1, 2, and 5 after the hepatectomy procedure. As a result, the ranking of gene expression stability value (M) of tested HKGs were as follows; GUSB > TFRC > RPL4 > HPRT1 > ACTB > GAPDH > PPIA, and TBP. This rank order data analysis indicated that PPIA and TBP were the most stable HKGs making them ideal for our quantitative analyses due to their lack of change during the liver regenerative time line (Fig. 2A).

In some cases, the normalization with two or more stable internal control reference genes may be required. Therefore, pairwise variations were calculated using geNorm for each data set to determine the optimal number of internal reference genes needed for normalization. In brief, the normalization factors (NF) were calculated for the most stable control genes (i.e., the lowest M value) and then other reference genes with the next lowest M values were added in a stepwise manner. Subsequently, pairwise variations of NF_n and NF_{n+1} were calculated, reflecting the effect of including additional ($n + 1$) genes [4]. From these analyses, two genes with most stable expression (TBP and PPIA) were found to be optimal for reliable normalization with a pairwise variation cut-off value of 0.15 (Fig. 2B). Below this cut-off value, there was no need to include an additional HKG, because the inclusion of a third gene had no significant effect on the pairwise variation.

Next, we used NormFinder, which was another algorithm to calculate the most stable HKGs in our set of 8 candidate HKGs [5]. The

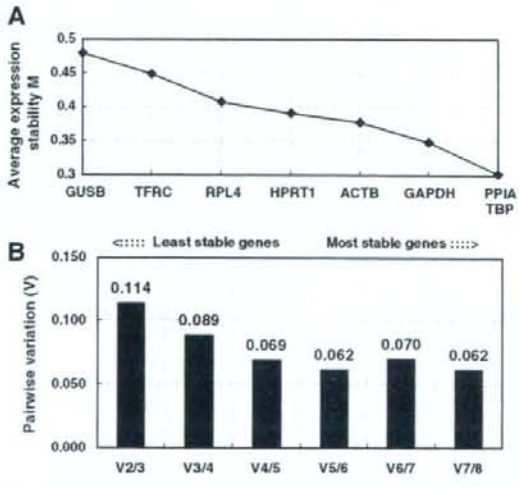

Fig. 2. (A) Average expression stability values (M) of 8 candidate housekeeping genes (HKGs). HKGs were graphed to illustrate the average gene expression stability (M) on the Y-axis, and its associated ranking from least to most stable expression (X-axis) as calculated by geNorm ($n = 50$ liver samples). Lower M value of average expression stability indicates more stable expression. (B) Determination of the optimal number of control genes for normalization. The optimal number of control genes for normalization was calculated on the basis of a pair-wise variation (V) analysis.

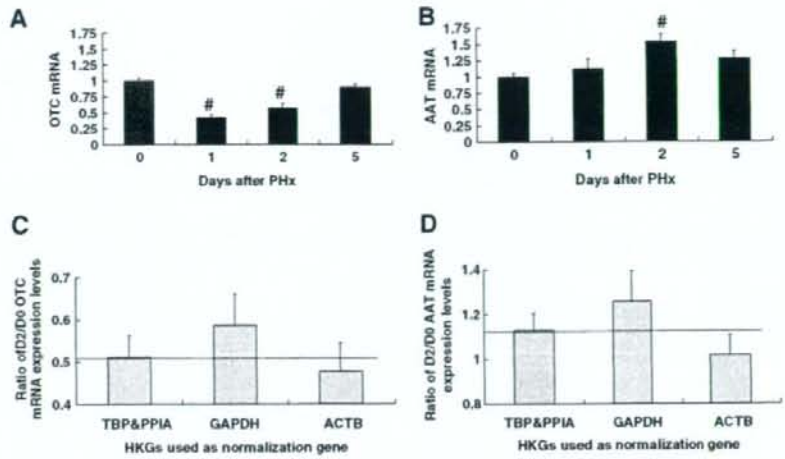

Fig. 3. Expression levels of two target genes, ornithine carbamoyltransferase (OTC) and α1-antitrypsin (AAT). (A and B) Non-normalized expression of two target genes transcribed in mouse livers during states of quiescence and active regeneration post-hepatectomy. The liver lobes removed at the time of hepatectomy were used as quiescent liver samples (day 0, $n = 25$). The remaining liver lobes were obtained 1, 2, or 5 days after hepatectomy and used as the proliferative liver samples ($n = 9$, 8, and 8, respectively). Data was expressed as a ratio to the day 0 liver samples and were represented as the mean ± SEM. $^{\#}P < 0.05$ vs day 0. (C and D) The gene expression levels of OTC and AAT were normalized to three different sets of HKGs (the geometric mean of PPIA and TBP, GAPDH, and ACTB). The normalized gene expression values were shown for the day 2 liver samples relative to the corresponding expression values at day 0 ($n = 8$). Data was represented as the mean ± SEM.

NormFinder was designed to calculate the stability by using the combined estimate of intra- and intergroup expression variations of the analyzed genes. The calculated stability values of the 8 candidate HKGs were as follows: GAPDH = 0.172; ACTB = 0.138; HPRT1 = 0.132; GUSB = 0.199; PPIA = 0.088; TBP = 0.118; TFRC = 0.167; and RPL4 = 0.142. Based on these values, the NormFinder program validated the findings with the geNorm algorithm, in which the most stable single gene was PPIA, and the best combination of the HKGs was PPIA and TBP.

Expression levels of target gene influenced by the choice of a normalization gene(s)

The expression profile of target genes can be markedly influenced depending on the choice of the normalization gene(s). The expression levels of the two target genes, ornithine carbamoyltransferase (OTC) and α1-antitrypsin (AAT), both of which are synthesized by liver, were assessed. We determined the non-normalized mRNA expression profile of OTC and AAT in the same liver samples used in the determination of the HKG expression profile. The expression of OTC genes was shown to be significantly suppressed 1 and 2 days after hepatectomy (Fig. 3A), whereas the AAT gene expression was upregulated 2 days after hepatectomy ($P < 0.05$ vs quiescent status) (Fig. 3B). The mRNA expression levels of the liver samples 2 days after hepatectomy were normalized against three different sets of HGK, specifically GAPDH, ACTB and the geometric mean of PPIA and TBP. Subsequently, the normalized day 2 values were divided by the normalized liver values obtained at day 0. As shown in Fig. 3C and D, though not significantly, both OTC and AAT mRNA levels that were normalized by the geometric mean of PPIA and TBP were lower than levels normalized by GAPDH, and higher than those normalized by ACTB. These results indicate that depending on which particular HKG was used in the normalization, the expression profile of the target gene can be influenced and produce different levels of gene expression.

Discussion

The appropriate choice of individual or a group of reference genes, in general endogenously expressed housekeeping genes (or HKGs), is critical in the quantification of gene expression profiles under different conditions, such as liver regeneration. In the present study, we examined 8 candidate HKGs that were selected in terms of their broad use in previously published studies using the liver and other type of tissues. The expression levels of the candidate HKG were assessed in quiescent or regenerating mouse livers at various stages of proliferation. The present results were based on geNorm and NormFinder analyses, which confirmed that the expression levels of the PPIA and TBP reference genes were the most stable among the 8 candidates regardless of the cell cycle status of the livers.

In the first 24 h following a partial hepatectomy in mice, hepatocyte DNA synthesis is initiated. Over the next 24 h period, the DNA synthesis phase become synchronized and peaks, and then slowly returns back to normal levels by day 5 after the hepatectomy. At day 5, the remnant liver lobes have undergone sufficient hyperplasia to return the liver weight back to its original pre-hepatectomy weight [2,13]. This rapid process from initiation to completion of the regeneration event prompted us to assess a panel of HKGs using liver samples harvested at day 1, 2, and 5 after the hepatectomy procedure.

In this present study, mRNA expression levels were upregulated in 6 out of 8 HKGs analyzed during the active phase of liver regeneration (days 1 and/or 2). The upregulation of these particular HKGs demonstrated that they likely play a vital role in the events related with DNA synthesis, cell division and hepatic growth. As an example, GAPDH and ACTB genes, which have been widely applied for the normalization of gene expression analysis of various types of tissues, showed significant increases in the mRNA expression at day 1 and/or 2 after hepatectomy (Fig. 1). The temporal upregulation of these two HKGs in the liver regeneration process were consistent with previous reports [14–16]. We have recently

showed that human hepatocytes undergoing active proliferation following transplantation into mouse liver exhibited higher GAPDH mRNA expression compared to normal human livers [17]. These data taken together, suggest that these two genes may not be appropriate reference genes to normalize target gene expression, particularly in the context of liver regeneration. Therefore, the identification of suitable internal reference genes that are not affected by a given experimental condition is critically important to accurately analyze expression levels of target genes. To address this problem, we utilized two different algorithms, geNorm and Normfinder [4,5], to select an optimal reference gene from a panel of candidate HKGs in quiescent and regenerating mouse livers. As a result, we found that the PPIA and TBP mRNA were most stably expressed, and both programs concluded that a combination of the two genes were the most appropriate for normalization of unknown target genes to determine their expression profiles in liver regeneration (Fig. 1). From examining the non-normalized RPL4 gene expression (Fig. 1), the values were found to be stable regardless of the time point. However, analyzing the expression data in a comprehensive manner using the two software programs demonstrated that the RPL4 reference gene was not stable. This is one example in which non-normalized data is only one method to demonstrate the potential reliability as a reference gene, but that other comparative analyses are needed, such as the geNorm and NormFinder, to further validate the suitability of selecting appropriate HKGs.

PPIA (peptidylprolyl isomerase A), also called as cyclophilin A, forms a ternary complex with cyclosporin A and the calcium-calmodulin-activated serine/threonine-specific protein phosphatase calcineurin [18]. This gene has been recently reported to be preferred over other commonly used HKGs following its analysis in various cell lines and tissues [19]. The other stably expressed reference gene, TBP (also known as TATA box binding protein), is a protein required by all three eukaryotic RNA polymerases to correctly initiate the transcription of ribosomal, messenger, small nuclear and transfer RNAs [20]. The usefulness of TBP gene has also been validated in other sets of experimental conditions [21]. Although there is a strong possibility that other more suitable reference genes other than the ones presently analyzed in our study, we have confirmed that PPIA and TBP genes gave us reliable and stable gene expression compared to other more commonly used HKGs, including ACTB or GAPDH (Fig. 3C and D).

The elucidation of liver regeneration events are further supported by recent studies in which hepatocyte-based approaches were developed, including liver tissue engineering [10,11,22], hepatocyte transplantation [23], hepatocyte propagation [17], and hepatic differentiation from stem cells [24]. Taken together, the results from the current study where we validated merit of normalizing target gene expression with the combined expression values of PPIA and TBP genes should serve as a viable method to accurately quantify gene expression profiles related with liver regeneration.

Acknowledgments

The authors thank Dr. Frank Park (Medical College of Wisconsin) for his critical reading of the manuscript. This study was supported by grants for AIDS Research from the Ministry of Health, Labor and Welfare of Japan (A.Y.), Special Coordination Funds for Promoting Science and Technology from the Ministry of Education, Culture, Sports, Science and Technology of Japan (K.O. and T.O.), Novartis Foundation Japan (K.O.), and Bayer Hemophilia Award Program (K.O.).

References

[1] N. Fausto, J.S. Campbell, K.J. Riehle, Liver regeneration, Hepatology 43 (2006) S45–S53.
[2] G.K. Michalopoulos, Liver regeneration, J. Cell. Physiol. 213 (2007) 286–300.
[3] S.A. Bustin, Quantification of mRNA using real-time reverse transcription PCR (RT-PCR): trends and problems, J. Mol. Endocrinol. 29 (2002) 23–39.
[4] J. Vandesompele, K. De Preter, F. Pattyn, B. Poppe, N. Van Roy, A. De Paepe, F. Speleman, Accurate normalization of real-time quantitative RT-PCR data by geometric averaging of multiple internal control genes, Genome Biol. 3 (2002). RESEARCH0034.
[5] C.L. Andersen, J.L. Jensen, T.F. Orntoft, Normalization of real-time quantitative reverse transcription-PCR data: a model-based variance estimation approach to identify genes suited for normalization, applied to bladder and colon cancer data sets, Cancer Res. 64 (2004) 5245–5250.
[6] Q. Gao, X.Y. Wang, J. Fan, S.J. Qiu, J. Zhou, Y.H. Shi, Y.S. Xiao, Y. Xu, X.W. Huang, J. Sun, Selection of reference genes for real-time PCR in human hepatocellular carcinoma tissues, J Cancer Res. Clin. Oncol. (2008).
[7] M. Jain, A. Nijhawan, A.K. Tyagi, J.P. Khurana, Validation of housekeeping genes as internal control for studying gene expression in rice by quantitative real-time PCR, Biochem. Biophys. Res. Commun. 345 (2006) 646–651.
[8] A.K. Greene, M. Puder, Partial hepatectomy in the mouse: technique and perioperative management, J. Invest. Surg. 16 (2003) 99–102.
[9] K. Ohashi, M.A. Kay, T. Yokoyama, H. Kuge, H. Kanehiro, M. Hisanaga, S. Ko, Y. Nakajima, Stability and repeat regeneration potential of the engineered liver tissues under the kidney capsule in mice, Cell Transplant. 14 (2005) 621–627.
[10] K. Ohashi, J.M. Waugh, M.D. Dake, T. Yokoyama, H. Kuge, Y. Nakajima, M. Yamanouchi, H. Naka, A. Yoshioka, M.A. Kay, Liver tissue engineering at extrahepatic sites in mice as a potential new therapy for genetic liver diseases, Hepatology 41 (2005) 132–140.
[11] K. Ohashi, T. Yokoyama, M. Yamato, H. Kuge, H. Kanehiro, M. Tsutsumi, T. Amanuma, H. Iwata, J. Yang, T. Okano, Y. Nakajima, Engineering functional two- and three-dimensional liver systems in vivo using hepatic tissue sheets, Nat. Med. 13 (2007) 880–885.
[12] T. Matsuo, S. Yamaguchi, S. Mitsui, A. Emi, F. Shimoda, H. Okamura, Control mechanism of the circadian clock for timing of cell division in vivo, Science 302 (2003) 255–259.
[13] K. Ohashi, F. Park, M.A. Kay, Role of hepatocyte direct hyperplasia in lentivirus-mediated liver transduction in vivo, Hum. Gene Ther. 13 (2002) 653–663.
[14] Y. Fukuhara, A. Hirasawa, X.K. Li, M. Kawasaki, M. Fujino, N. Funeshima, S. Katsuma, S. Shiojima, M. Yamada, T. Okuyama, S. Suzuki, G. Tsujimoto, Gene expression profile in the regenerating rat liver after partial hepatectomy, J. Hepatol. 38 (2003) 784–792.
[15] Y. Ito, H. Hayashi, M. Taira, M. Tatibana, Y. Tabata, K. Isono, Depression of liver-specific gene expression in regenerating rat liver: a putative cause for liver dysfunction after hepatectomy, J. Surg. Res. 51 (1991) 143–147.
[16] Y. Kurumiya, K. Nozawa, K. Sakaguchi, M. Nagino, Y. Nimura, S. Yoshida, Differential suppression of liver-specific genes in regenerating rat liver induced by extended hepatectomy, J. Hepatol. 32 (2000) 636–644.
[17] K. Tatsumi, K. Ohashi, M. Kataoka, C. Tateno, M. Shibata, H. Naka, M. Shima, M. Hisanaga, H. Kanehiro, T. Okano, K. Yoshizato, Y. Nakajima, A. Yoshioka, Successful in vivo propagation of factor IX-producing hepatocytes in mice. Potential for cell-based therapy in haemophilia B, Thromb. Haemost. 99 (2008) 883–891.
[18] P. Wang, J. Heitman, The cyclophilins, Genome Biol. 6 (2005) 226.
[19] M. Nishimura, T. Nikawa, Y. Kawano, M. Nakayama, M. Ikeda, Effects of dimethyl sulfoxide and dexamethasone on mRNA expression of housekeeping genes in cultures of C2C12 myotubes, Biochem. Biophys. Res. Commun. 367 (2008) 603–608.
[20] S.K. Burley, The TATA box binding protein, Curr. Opin. Struct. Biol. 6 (1996) 69–75.
[21] M. Jung, A. Ramankulov, J. Roigas, M. Johannsen, M. Ringsdorf, G. Kristiansen, K. Jung, In search of suitable reference genes for gene expression studies of human renal cell carcinoma by real-time PCR, BMC Mol. Biol. 8 (2007) 47.
[22] K. Ohashi, P.L. Marion, H. Nakai, L. Meuse, J.M. Cullen, B.B. Bordier, R. Schwall, H.B. Greenberg, J.S. Glenn, M.A. Kay, Sustained survival of human hepatocytes in mice. A model for in vivo infection with human hepatitis B and hepatitis delta viruses, Nat. Med. 6 (2000) 327–331.
[23] K. Tatsumi, K. Ohashi, M. Shima, Y. Nakajima, T. Okano, A. Yoshioka, Therapeutic effects of hepatocyte transplantation on hemophilia B, Transplantation (2008).
[24] S. Kasuda, A. Kubo, Y. Sakurai, S. Irion, K. Ohashi, K. Tatsumi, Y. Nakajima, Y. Saito, K. Hatake, S.W. Pipe, M. Shima, A. Yoshioka, Establishment of embryonic stem cells secreting human factor VIII for cell-based treatment of hemophilia A, J. Thromb. Haemost. (2008).

Journal of Thrombosis and Haemostasis, 6: 1352–1359 DOI: 10.1111/j.1538-7836.2008.03022.x

ORIGINAL ARTICLE

Establishment of embryonic stem cells secreting human factor VIII for cell-based treatment of hemophilia A

S. KASUDA*†‡, A. KUBO§, Y. SAKURAI*, S. IRION¶, K. OHASHI**[1], K. TATSUMI*, Y. NAKAJIMA**, Y. SAITO§, K. HATAKE†, S. W. PIPE‡‡, M. SHIMA* and A. YOSHIOKA*

*Department of Paediatrics, Nara Medical University, Kashihara, Nara; †Department of Legal Medicine, Nara Medical University, Kashihara, Nara; ‡Department of Legal Medicine, Hyogo College of Medicine, Nishinomiya, Hyogo; §First Department of Internal Medicine, Nara Medical University, Kashihara, Nara, Japan; ¶Department of Gene and Cell Medicine, Mount Sinai School of Medicine, New York, NY, USA; **Department of Surgery, Nara Medical University, Kashihara, Nara, Japan; and ‡‡Department of Pediatrics, University of Michigan Medical Center, Ann Arbor, MI, USA

To cite this article: Kasuda S, Kubo A, Sakurai Y, Irion S, Ohashi K, Tatsumi K, Nakajima Y, Saito Y, Hatake K, Pipe SW, Shima M, Yoshioka A. Establishment of embryonic stem cells secreting human factor VIII for cell-based treatment of hemophilia A. *J Thromb Haemost* 2008; **6**: 1352–9.

Summary. *Background:* Hemophilia A is an X-chromosome-linked recessive bleeding disorder resulting from an *F8* gene abnormality. Although various gene therapies have been attempted with the aim of eliminating the need for factor VIII replacement therapy, obstacles to their clinical application remain. *Objectives:* We evaluated whether embryonic stem (ES) cells with a tetracycline-inducible system could secrete human FVIII. *Methods and results:* We found that embryoid bodies (EBs) developed under conditions promoting liver differentiation efficiently secreted human FVIII after doxycycline induction. Moreover, use of a B-domain variant *F8* cDNA (226aa/N6) dramatically enhanced FVIII secretion. Sorting based on green fluorescent protein (GFP)–brachyury (Bry) and c-kit revealed that GFP–Bry^+/$c\text{-}kit^+$ cells during EB differentiation with serum contain an endoderm progenitor population. When GFP–Bry^+/$c\text{-}kit^+$ cells were cultured under the liver cell-promoting conditions, these cells secreted FVIII more efficiently than other populations tested. *Conclusion:* Our findings suggest the potential for future development of an effective ES cell-based approach to treating hemophilia A.

Keywords: cell-based therapy, embryonic stem cells, factor VIII, hemophilia A.

Correspondence: Atsushi Kubo, First Department of Internal Medicine, Nara Medical University, 840 Shijo, Kashihara, Nara 634-8522, Japan.
Tel.: +81 744 22 3051 ext. 3411; fax: +81 744 22 9726.
E-mail: akubo@naramed-u.ac.jp

[1]Present address: Institute of Advanced Biomedical Engineering and Science, Tokyo Women's Medical University, Tokyo, Japan

Received 24 October 2007, accepted 25 April 2008

Introduction

Hemophilia A is an X-chromosome-linked recessive bleeding disorder resulting from an inversion or mutation within the *F8* gene, and is the most common of the congenital bleeding disorders [1]. The clinical severity of hemophilia A correlates closely with circulating levels of factor VIII (FVIII) protein. Current standard therapy for hemophilia A patients is replacement therapy with intravenous infusion of plasma-derived or recombinant FVIII concentrates [2]. However, the half-life of infused FVIII is short (10–12 h), and the cost of the frequent infusions necessary to maintain adequate plasma levels of FVIII is extremely high. Consequently, the development of a novel therapy leading to constitutive supply of FVIII is much desired in the next stage of the treatment of hemophilia. For that reason, gene therapy for hemophilia has received a great deal of attention [3]. Constant and sustained FVIII synthesis mediated by gene therapy in patients would obviate the risk of spontaneous bleeding without the need for repeated FVIII infusions. Although the gene therapy approach has shown promise in a mouse model [4], some drawbacks, such as hepatic damage or viral contamination in the non-motile sperm, have been reported [5,6].

As another approach, orthotopic liver transplantation (OLT) has also been attempted for the treatment of hemophilia [7]. Moreover, recent studies have shown that transplantation of hepatocytes [8] or sinusoidal endothelial cells [9] corrects the hemophilia A phenotype in mice, suggesting that cell-based therapy using primary cultured cells may be a useful approach to treating hemophilia. However, a disadvantage of these therapies is that there is a shortage of donors for transplantation or cell isolation.

Given the limitations of all the aforementioned therapies, we evaluated the potential of a cell-based therapy that makes use of embryonic stem (ES) cells as the source of active human FVIII. ES cells retain their totipotential capacity when

maintained on mouse embryonic feeder (MEF) cells and are able to spontaneously differentiate and generate various lineages via the embryoid body (EB) stage. We hypothesized that ES cell-based therapy would have unique characteristics that would enable us to overcome the problems associated with gene therapy or primary cultured cell transplantation. First, ES cells can provide a cell source with unlimited expansion capacity, thereby overcoming the shortage of donors for OLT or primary cultured cell transplantation. Second, hepatic damage or the contamination in the non-motile sperm fraction by viral vectors would be avoided, as there is no virus present.

In this study, to induce the human *F8* gene in ES cells, we used an ES cell line (Ainv18) that enables the inducible expression of the *F8* gene under the control of a tet-inducible promoter [10]. Although Ainv18 ES cells have been used previously for functional analysis of the transcriptional factors HoxB4 and Hex [10,11], we used them for synthesis of a secretable protein. Together, these advantageous features could make ES cell-based therapy an effective approach to the treatment of hemophilia A. Our aim in the present study, therefore, was to establish an ES cell line capable of doxycycline (Dox)-inducible *F8* gene expression and to determine the most suitable differentiation conditions for secretion of FVIII. We show that ES cells can secrete FVIII with antigen and coagulant activity, suggesting that ES cell-based therapy may be a potentially useful approach to treating hemophilia A.

Materials and methods

Growth and differentiation of ES cells

The cDNA construct harboring the full-length human wild-type (WT)-*F8* was described previously [12], as were the B-domain-deleted (BDD)-*F8* and 226aa/N6 cDNAs [13]. Ainv18 ES cells (a kind gift from M. Kyba and G. Q. Daley) were transfected with the WT-*F8*-plox, BDD-*F8*-plox or 226aa/N6-plox targeting plasmids by electroporation, yielding tet-WT-*F8*, tet-BDD-*F8* and tet-226aa/N6 ES cells, after which the transfectants were selected with G418, as described previously [11]. Green fluorescent protein (GFP)–brachyury (Bry) Ainv18 ES cells (S. Irion *et al.*, unpublished data) were established by targeting GFP to the Bry locus in Ainv18 ES cells [14].

ES cells were maintained on MEF cells and were passaged twice on gelatin-coated dishes before EB formation, as previously described [15]. To generate EBs, ES cells were dissociated to a single cell suspension with 0.25% trypsin/EDTA and cultured at various concentrations ($1–8 \times 10^3$ cells mL^{-1}) in 60-mm Petri-grade dishes in serum-containing differentiation medium [Iscoves' modified Dulbecco's medium (IMDM) supplemented with penicillin–streptomycin, 2 mM glutamine (Gibco/BRL, Grand Island, NY, USA), 0.5 mM ascorbic acid (Sigma-Aldrich, St Louis, MO, USA), 0.45 mM monothioglycerol (MTG; Sigma-Aldrich), 15% fetal bovine serum (FBS; Vitromex, Geilenkirchen, Germany), 5% protein-free hybridoma medium (Gibco/BRL) and 200 μg mL^{-1} transferrin (Boehringer Mannheim, Indianapolis, IN, USA)]. Cultures were maintained in a humidified chamber in a 5% CO_2/air mixture at 37 °C.

The experimental protocol is depicted schematically in Fig. 1A. When EBs were cultured in differentiation medium for 6 days, EBs differentiated into the mesodermal lineage, which includes mainly hematopoietic and endothelial cell populations (hematopoietic-like EBs). For liver differentiation, EBs were cultured in differentiation medium for 3 days and then transferred to serum replacement (SR) medium [IMDM supplemented with 15% knockout SR (Gibco/BRL), penicillin–streptomycin, 2 mM glutamine, 0.5 mM ascorbic acid, 0.45 mM MTG] and cultured for an additional 7 days. On day 10, the EBs were harvested and replated in 12-well tissue culture dishes coated with Matrigel (Becton Dickenson, San Jose, CA, USA) in IMDM with 15% FBS and 1 μM dexamethasone (Dex; Sigma-Aldrich), which led to the development of liver-like EBs [15].

Undifferentiated ES cells were passaged twice on gelatin. Hematopoietic-like EBs cultured with serum for 6 days were replated on 12-well culture dishes coated with Matrigel in IMDM with 15% FBS and 1 μM Dex for 2 days. Undifferentiated ES cells, day 8 hematopoietic-like EBs and day 13 liver-like EBs were stimulated with Dox for 2 days before assay. For *in vitro* assay of FVIII, the culture media were replaced with 500 μL of serum-free IMDM medium containing 5 mg mL^{-1} bovine serum albumin (Calbiochem, San Diego, CA, USA) [16] with or without human FVIII-free von Willebrand factor (VWF; Haematologic Technologies, Essex Junction, VT, USA). Twenty-four hours later, the supernatant and cell samples were harvested for determination of FVIII activity (FVIII:C) and FVIII antigen (FVIII:Ag) or protein levels.

Gene expression

For gene-specific reverse transcription polymerase chain reaction (RT-PCR), total RNA was extracted using RNeasy mini-kits and treated with RNase-free DNase (Qiagen, Valencia, CA, USA). One microgram of total RNA was reverse-transcribed into cDNA using a Superscript RT kit (Invitrogen, Carlsbad, CA, USA) with random hexamers. PCR was carried out using Taq polymerase (Takara Bio, Shiga, Japan) in PCR buffer, 2.5 mM $MgCl_2$, and 0.2 mM dNTPs. The primers for human specific *F8* were 5′-AGAGTTCCAAGCCTCCAACA-3′ (sense) and 5′-TAGACCTGGGTTTTCCATCG-3′ (antisense). The cycling protocol entailed one cycle of 94 °C for 5 min, followed by 25–35 cycles of denaturation at 94 °C for 1 min, annealing at 60 °C for 30 s and elongation at 72 °C for 1 min, and a final incubation at 72 °C for 7 min. Oligonucleotides for *Rex1*, *Gata1*, *Albumin1* (*Alb*), *transthyretin* (*Ttr*), *tyrosine aminotransferase* (*Tat*), *α-fetoprotein* (*Afp*), *Foxa2*, *Sox17*, *Cereberus*, *E-cadherin* (*E-cad*), *Hex* and *β-actin* have been previously described [15,17]. Quantitative real-time RT-PCR analysis was performed with an Applied Biosystems Prism 7700 Sequence Detection System using TaqMan® universal PCR master mix according to the manufacturer's specifications (Applied Biosystems, Foster City, CA, USA).

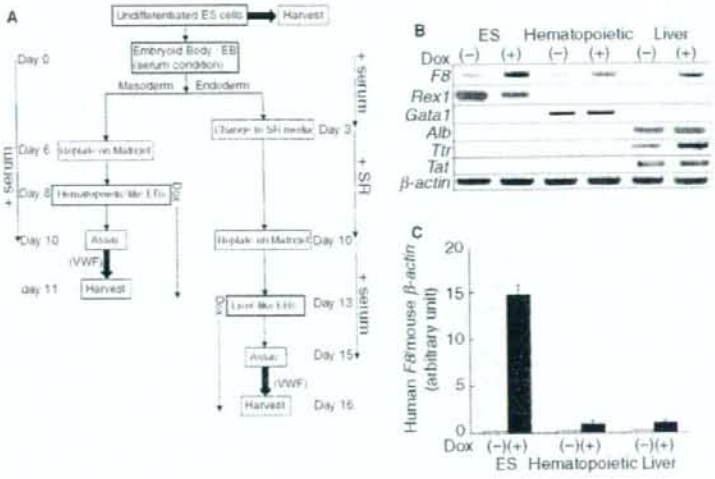

Fig. 1. Expressions of WT-*F8* mRNA by doxycycline (Dox) stimulation in undifferentiated embryonic stem (ES) cells, hematopoietic-like embryoid bodies (EBs) and liver-like EBs. (A) Schema of the experimental protocol. (B) Reverse transcription polymerase chain reaction (RT-PCR) analysis of variable marker genes in undifferentiated tet-WT-*F8* ES cells, hematopoietic-like EBs and liver-like EBs with or without Dox induction (1 μg mL^{-1}). (C) Real-time PCR analysis of *F8* mRNA levels in undifferentiated tet-WT-*F8* ES cells, hematopoietic-like EBs and liver-like EBs with or without Dox induction (1 μg mL^{-1}). The data presented are means of three independent experiments; the error bars represent the SEM. VWF, von Willebrand factor; SR, serum replacement.

The TaqMan probes and primers for human *F8* (assay identification number Hs00240767) and mouse *F8* (assay identification number Mm00433174) were assay-on-demand gene expression products (Applied Biosystems). The mouse *β-actin* gene (assay identification number Mm00607939) was used as an endogenous control.

FVIII assay

FVIII:C was measured in a one-stage activated partial thromboplastin time (APTT) clotting assay in a coagulometer (KC10A; Amelung, Lemgo, Germany) using human FVIII-deficient plasma (George King Biomedical, Overland Park, KS, USA). Activated partial thromboplastin and $CaCl_2$ were purchased from bioMerieux (Durham, NC, USA). FVIII:Ag was quantified using human FVIII-specific enzyme-linked immunosorbent assay (ELISA) kits (FVIII:C-EIA, Affinity Biologicals, Ancaster, ON, Canada), according to the manufacturer's instructions. These ELISA kits employ FVIII light chain specific antibody, and is the same kits used for 226aa/N6 detection previously [13]. For measurement of both FVIII:C and FVIII:Ag, a standard curve was generated using normal human plasma (Coagtrol N; Sysmex, Kobe, Japan) in serial doubling dilutions (1 : 10 to 1 : 1280) in 0.05 M imidazole saline buffer. Each supernatant sample was applied to these assays without dilution rather than 10× dilution. Therefore, FVIII:C and FVIII:Ag levels of culture supernatant samples should be considered as 1/10 of the raw data. We calculated FVIII:Ag levels in normal human plasma as 1 nM. The detection limits of the FVIII:C and FVIII:Ag assays were 10 mIU mL^{-1} and 10 pM, respectively. The attached cell samples in each well were also harvested to determine the amount of protein by a BCA protein assay (Pierce Biotechnology, Rockford, IL, USA). Although these types of data are typically signified in terms of cell number, it is very difficult to count cell numbers in liver-like EBs, due to formation of tight aggregates. In order to adjust secretion levels from the equal protein levels of EBs, FVIII:C and FVIII:Ag levels in the supernatant of each well were adjusted by protein amount of attached cells in the same well. Data are shown as 'not detected' when the raw data for FVIII:C and FVIII:Ag were under the detection limit of the assays (10 mIU mL^{-1} and 10 pM, respectively).

Cell sorting

Day 3.5 EBs were dissociated with trypsin–EDTA, stained with anti-mouse c-kit-phycoerythrin (BD PharMingen, San Diego, CA, USA) in IMDM supplemented with 5% FBS, and sorted in a FACS Aria cell sorter (Becton Dickinson). After sorting, the cells were reaggregated in SR medium and cultured using the liver differentiation protocol.

Results

Tet-WT-F8 ES cells secrete active human FVIII protein

Using the Ainv18 ES cell line, we established ES cells in which the *F8* gene was induced by the tetracycline analog Dox (tet-WT-*F8* ES cells). Tet-WT-*F8* ES cells were cultured such that

we were able to obtain three different cell types: undifferentiated ES cells, enriched hematopoietic EBs (hematopoietic-like EBs), and enriched liver EBs (liver-like EBs). RT-PCR analysis revealed that tet-WT-*F8* ES cells were well differentiated under hematopoietic cell-promoting conditions (hematopoietic conditions) or liver cell-promoting conditions (liver conditions; Fig. 1B), which is consistent with earlier findings [15]. *Rex1* and *Gata1* are marker genes for undifferentiated ES cells and hematopoietic cells, respectively. *Alb*, *Ttr* and *Tat* are marker genes for liver cells. Recently, we further confirmed that liver-like EBs also secreted albumin and transferrin (A. Kubo, unpublished data). Addition of Dox (1 μg mL^{-1}) to the culture medium successfully upregulated *F8* mRNA expression under all three differentiation conditions (Fig. 1B). We also quantitatively analyzed mRNA expression by real-time PCR (Fig. 1C). Interestingly, *F8* mRNA levels in undifferentiated ES cells were much higher than those in hematopoietic-like EBs and liver-like EBs. The reason for this is currently unclear. However, we deduce that gene induction by Dox may be more effective in undifferentiated ES cells than in the other differentiated EBs because of the three-dimensional structure of EBs. On the other hand, *F8* mRNA expression levels of the two cell types were found to be identical. Mouse *F8* mRNA was not induced in liver-like EBs (data not shown). Among the different cell types, FVIII:C and FVIII:Ag were detected only in the supernatant from liver-like EBs; neither was detected with undifferentiated ES cells or hematopoietic-like EBs (Fig. 2A,B). Apparently, the differentiation conditions and the resulting cell types are critical to the production and secretion of FVIII, despite the mRNA levels induced by Dox. In the presence of 2.5 μg mL^{-1} of VWF, Dox-induced levels of both FVIII:C and FVIII:Ag were increased to about twice that seen in the absence of VWF (data not shown). Accordingly, VWF was added at a concentration of 2.5 μg mL^{-1} in subsequent experiments. We also assessed the effect of Dox concentrations on FVIII secretion. When liver-like EBs were stimulated with various concentrations of Dox, the level of *F8* mRNA increased in a dose-dependent manner with increasing

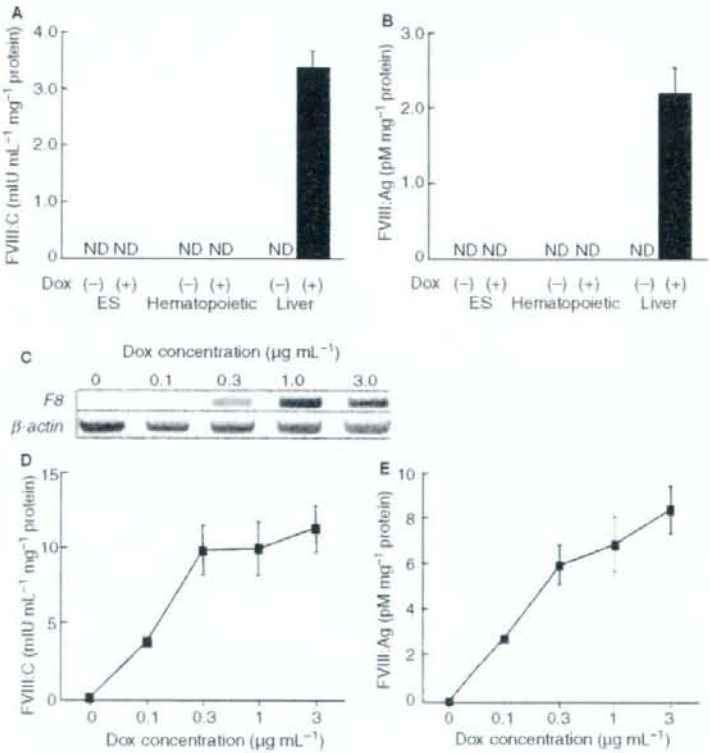

Fig. 2. FVIII:C and FVIII:Ag levels in undifferentiated embryonic stem (ES) cells, hematopoietic-like embryoid bodies (EBs) and liver-like EBs with or without doxycycline (Dox) stimulation. (A, B) FVIII:C (A) and FVIII:Ag (B) levels in media conditioned by cells cultured under the three differentiation conditions, with or without Dox induction (1 μg mL^{-1}). No von Willebrand factor (VWF) was added. (C) *F8* mRNA expression induced by the indicated concentrations of Dox from tet-WT-*F8* ES cells. (D, E) Secretion of FVIII:C (D) and FVIII:Ag (E) from tet-WT-*F8* ES cells induced by the indicated concentrations of Dox in the presence of 2.5 μg mL^{-1} VWF. The data presented are means of three independent experiments; the error bars represent the SEM. ND, not detected.

Dox concentrations (Fig. 2C), and there were corresponding increases in both FVIII:C and FVIII:Ag (Fig. 2D,E).

Tet-226aa/N6 ES cells secrete active FVIII more efficiently than tet-WT-F8 ES cells

Earlier reports showed that BDD-*F8* is more efficient than WT-*F8* for FVIII production, because higher mRNA levels are achieved [18,19]. In addition, Miao *et al.*[13] bioengineered a BDD-*F8* variant with 226 amino acids of the native *F8* B-domain that includes six asparagine-linked glycosylations (226aa/N6). They showed that COS-1 or CHO cells transfected with 226aa/N6 secrete active FVIII more efficiently than WT-*F8*- or BDD-*F8*-expressing cells. To evaluate these three *F8* types with respect to FVIII production and secretion, tet-WT-*F8* ES cells, tet-BDD-*F8* ES cells and tet-226aa/N6 ES cells were cultured under the liver conditions. Real-time PCR analysis showed that BDD-*F8* mRNA was expressed 2-fold higher than WT-*F8*, and 226aa/N6 mRNA levels were between those of WT-*F8* and BDD-*F8* (Fig. 3A). These results suggest that the length of the B-domain may affect the transcriptional levels of the *F8* gene.

FVIII secretion in liver-like EBs from tet-BDD-*F8* ES cells was about 1.5-fold higher than in those from tet-WT-*F8* ES cells (Fig. 3B,C). Furthermore, FVIII secretion in liver-like EBs from tet-226aa/N6 ES cells was about 6–10-fold higher than in those from tet-WT-*F8* ES cells (Fig. 3B,C). These results demonstrated that the construct of 226aa/N6 efficiently produced higher levels of *F8* regardless of transcriptional levels.

Comparison of FVIII secretion in population sorting based on the Bry/c-kit

Recently, Gouon-Evans *et al.* showed that activin can induce definitive endoderm in the absence of serum and that the GFP–Bry$^+$/c-kit$^+$ population was the definitive endoderm progenitor under this condition [20]. We tested whether the GFP–Bry$^+$/c-kit$^+$ population cultured in the presence of serum also contained endoderm progenitors, and which subpopulation gave rise to FVIII-secreting cells. Tet-226aa/N6 ES cells were differentiated for 3.5 days in the presence of serum, at which time the GFP–Bry$^+$ and c-kit$^+$ populations had been induced (Fig. 4A). On the basis of earlier studies [14,20], the GFP–Bry$^+$/c-kit$^-$ and GFP–Bry$^+$/c-kit$^+$ cell fractions were deemed to be mesoderm and endoderm, respectively. After the population was sorted and harvested for RNA isolation, RT-PCR showed that *Foxa2* and *Sox17*, which are normally expressed in endoderm, were expressed primarily in GFP–Bry$^+$/c-kit$^+$ cells (Fig. 4B). *Cereberus* and *E-cad*, which are expressed in ES cell-derived endoderm [17], and *Hex*, which is an important transcriptional factor for liver specification [21], were also strongly expressed in the GFP–Bry$^+$/c-kit$^+$ fraction. Taken together, these results suggest that GFP–Bry$^+$/c-kit$^+$ cells cultured in the presence of serum contained the definitive endoderm population.

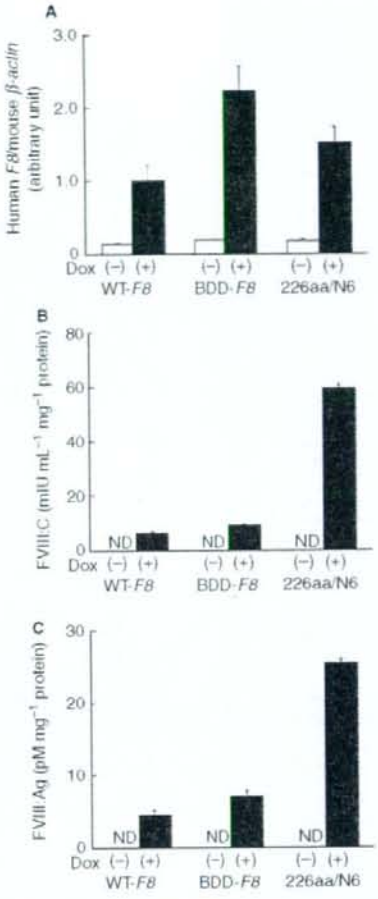

Fig. 3. FVIII secretion from tet-WT-*F8*, tet-BDD-*F8* and tet-226aa/N6 ES cells differentiated under the liver conditions. (A) Real-time PCR analysis of *F8* mRNA levels in tet-WT-*F8*, tet-BDD-*F8* and tet-226aa/N6 ES cells; note that doxycycline (Dox) (1 μg mL^{-1}) induced the highest levels of *F8* mRNA expression in BDD-*F8* cells. (B, C) Secretion of FVIII:C (B) and FVIII:Ag (C) from tet-WT-*F8*, BDD-*F8* and 226aa/N6 ES cells in the presence of 2.5 μg mL^{-1} von Willebrand factor, with or without Dox (1 μg mL^{-1}) induction. The data presented are means of three independent experiments; the error bars represent the SEM. ND, not detected; WT, wild type; BDD, B-domain-deleted.

After sorting, each of the populations derived from tet-226aa/N6 ES cells was reaggregated in SR medium and cultured under the liver conditions. On day 15, EBs derived from GFP–Bry$^+$/c-kit$^+$ cells expressed *Afp* and *Alb* mRNA more strongly than either presorted or GFP–Bry$^+$/c-kit$^-$ cells (Fig. 4C). We then examined the cell populations responsible for the FVIII secretion, and we found that EBs derived from the GFP–Bry$^+$/c-kit$^+$ population were more active for FVIII secretion than the presorted EBs following induction with Dox (Fig. 4D,E). By contrast, GFP–Bry$^-$